https://doi.org/10.5194/egusphere-2026-3151
Preprint. Discussion started: 24 June 2026
© Author(s) 2026. CC BY 4.0 License.

Groundwater-Level Response of Annual CO_2 Budgets from a Dutch Eddy Covariance Network: Comparison with European Temperate Peatlands across Land Use and Sites

Laurent Bataille[1], Bart Kruijt[1], Alexander Buzacott[2,7], Wilma Jans[1], Wietse Franssen[1], Jan Biermann[1], Hanne Berghuis[1], Quint van Giersbergen[3], Tom Heuts[5], Reinder Nouta[4], Niek Bosma[4], Ron Lootens[2], Hong Zhao[1], Merit van den Berg[2,6], Ype van de Velde[2], Christian Fritz[3], Gilles Erkens[8], and Ronald Hutjes[1]

[1]Earth Systems and Global Change Group, Wageningen University, Wageningen, the Netherlands
[2]Earth and Climate, Vrije Universiteit, Amsterdam, the Netherlands
[3]Aquatic Ecology and Environmental Biology, Radboud Universiteit, Nijmegen, the Netherlands
[4]Wetterskip Fryslân, Leeuwarden, the Netherlands
[5]Department of Ecology, Radboud Institute for Biological and Environmental Sciences, Radboud University, Nijmegen, the Netherlands
[6]UK Centre for Ecology & Hydrology, Wallingford, United Kingdom
[7]Institute for Atmospheric and Earth System Research (INAR)/Physics, Faculty of Science, University of Helsinki, Helsinki, Finland
[8]Subsurface and Groundwater Systems Unit, Deltares Research Institute, Utrecht, the Netherlands

Correspondence: Bart Kruijt (bart.kruijt@wur.nl) and Ronald Hutjes (ronald.hutjes@wur.nl)

Abstract. Peatlands in the Netherlands hold significant cultural, agricultural, and ecological value but also contribute substantially to national greenhouse gas (GHG) emissions as a result of drainage. This necessitates urgent mitigation, leading to the implementation of various land and water management strategies. As part of the Dutch national GHG research program (NOBV), eddy covariance (EC) measurements of carbon dioxide (CO_2) fluxes were conducted at 20 sites, encompassing managed peat meadows, wet nature areas, and paludiculture systems over periods of 1 to 3 years. A novel mobile EC set-up was utilized at some locations to enhance spatial coverage.

Net Ecosystem Exchange (NEE) of CO_2 demonstrated pronounced seasonal dynamics across different land-use types. Wet and highly productive systems exhibited both elevated uptake and emissions, leading to intervals of net CO_2 uptake. Managed pastures were typically net emitters on a daily timescale, except during early summer when assimilation peaked. Although annual net ecosystem carbon balance (NECB) estimates were subject to uncertainty due to data gaps and adjustments for harvest, grazing, and manure application, systematic differences between land-use types remained evident. To assess the sensitivity of CO_2 emissions to groundwater dynamics, ecological response functions (ERFs) were employed to relate NECB to groundwater depth, and these relationships were compared with findings from the literature. Across all sites, NECB exhibited only a weak association with mean annual groundwater level when referenced to the soil surface (ERF slope approximately 0.5 t CO_2 ha^{-1} yr^{-1} cm^{-1}, $R^2 = -0.08$), and an even weaker association with mean summer groundwater level. When groundwater depth was referenced to the clay layer, the inferred ERF sensitivity increased, resulting in steeper slopes of about 0.8 t CO_2 ha^{-1} yr^{-1} cm^{-1} ($R^2 = 0.26$), although the overall explanatory power remained limited. These ERF-based sensitiv-

https://doi.org/10.5194/egusphere-2026-3151
Preprint. Discussion started: 24 June 2026
© Author(s) 2026. CC BY 4.0 License.

ities align with previously published ERFs, including studies that report non-linear groundwater–CO_2 responses and threshold behavior.

Groundwater management interventions produced mixed effects on NECB. Of the pasture-oriented measures, only the Active Water Infiltration System (AWIS) resulted in a detectable shift in NECB beyond background interannual variability, while other interventions were not distinguishable from within–land-use variability. By contrast, clearer categorical patterns emerged across land-use and soil classes: restored wetlands and paludiculture systems showed lower net CO_2 emissions than drained managed grasslands, and sites with a clay cap consistently emitted less CO_2 than pure peat under comparable management. Overall, these results indicate that although mean groundwater metrics have limited predictive power at the site-year level, CO_2 emissions at landscape scales are primarily governed by land use and the presence of a clay-layer, which defines the baseline against which water-management measures operate.

1 Introduction

Dutch peatlands, remnants of a post-glacial fens and bogs once spanning from Flanders to Denmark (Erkens et al., 2016; Vos et al., 2020), have been largely converted into polders and dairy pastures over the past two millennia (Woestenburg and Kwakernaak, 2009). Drainage has made these soils major carbon dioxide (CO_2) emitters, responsible for about 3% of national greenhouse gas emissions (Arets et al., 2023). Under the Paris and National Climate Agreements, the Netherlands aims to cut peatland emissions by 1 Mt CO_2-eq annually by 2030 (Ministerie van Economische Zaken en Klimaat, 2019), requiring coordinated efforts to raise groundwater levels and slow peat oxidation (Schrier-Uijl et al., 2014; Erkens et al., 2022). Mitigation options include subsurface infiltration, clay amendments (van Agtmaal et al., 2025), ditch water level adjustments, and wet land-use transitions such as paludiculture (Pijlman et al., 2020; Wils et al., 2025). Broader transitions to inundated systems such as constructed wetlands are also being considered, motivated by the high costs of water pumping (Sen et al., 2023) and the increasing need for water retention in the landscape (Zingstra and Vertegaal, 2021). Although the potential benefits and trade-offs of these approaches are increasingly recognized, their effectiveness in reducing greenhouse gas emissions has been increasingly quantified in recent years, though systematic evidence across the full range of management types remains limited (van den Akker et al., 2010, 2012; Couwenberg, 2018; Evans et al., 2021; Weideveld et al., 2021; Aben et al., 2024). In fen meadows, groundwater management plays a crucial role in peat degradation and greenhouse gas (GHG) emissions. When peatlands are drained, the resulting aeration within soil promotes aerobic decomposition, leading to increased CO_2 emissions (Tiemeyer et al., 2016; Schrier-Uijl et al., 2014). Consequently, drainage can transition peatlands from carbon sinks to significant CO_2 sources. Several ecosystem response functions (ERFs) have been developed to describe the relationship between annual water table depth, peat oxidation, and methane emissions (Jurasinski et al., 2016; Evans et al., 2021; Tiemeyer et al., 2020).

The most commonly used ERFs state that peat oxidation follows a linear trend regarding the groundwater level— each centimeter of exposed peat generates between 300 kg and 500 kg CO_2 per hectare annually (Jurasinski et al., 2016; Evans et al., 2021; Aben et al., 2024). Alternatively, commonly used approaches adopt non-linear ERFs, whereby capturing emissions

https://doi.org/10.5194/egusphere-2026-3151
Preprint. Discussion started: 24 June 2026
© Author(s) 2026. CC BY 4.0 License.

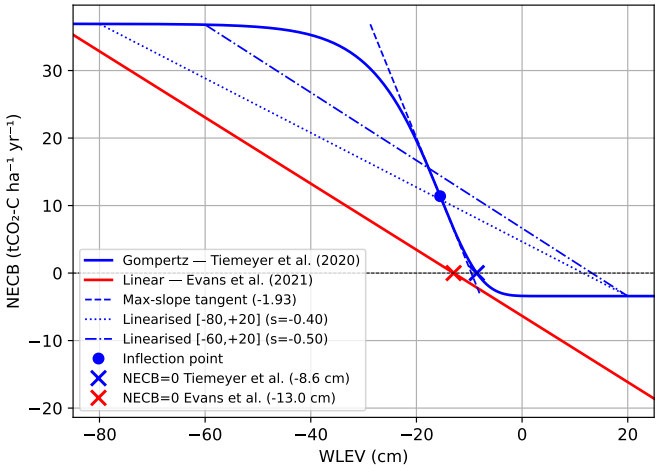

Fig. 1. Comparison of the two main families of emission response functions (ERFs) linking annual NECB to groundwater level (WLEV), based on published relationships. The linear ERF (red; (Evans et al., 2021)) assumes a constant NECB increase per centimeter of exposed peat, with zero emission at -13 cm. The Gompertz ERF (blue solid; (Tiemeyer et al., 2020)) captures a non-linear, phase-dependent response with an inflection point of maximum sensitivity at approximately -16 cm and saturation at deeper drainage. The dashed tangent indicates the maximum Gompertz slope ($s = -1.93$ $\mathrm{t_{CO_2}\ ha^{-1}\ yr^{-1}\ m_{bgl}^{-1}}$). The dotted and dash-dot lines show the effective linear slopes of the Gompertz curve over the $[-80, +20]$ cm ($s = -0.40$) and $[-60, +20]$ cm ($s = -0.50$) groundwater intervals, respectively, corresponding to the slope columns reported in Table 2. Zero-emission groundwater levels (NECB $= 0$) are marked for each ERF. The contrast between the maximum Gompertz slope and its interval-averaged values illustrates why the choice of groundwater depth range strongly influences the ERF slope reported in the literature.

caused by deeper soil drainage is the primary motivation for introducing this non-linearity. These ERFs detail a saturation effect due to limited oxygen availability at greater peat depth, typically using Gompertz functions (Tiemeyer et al., 2020; Koch et al., 2023). At near-surface groundwater conditions, some models additionally couple CO_2 and CH_4 emissions through a transfer depth, above which CH_4 becomes the dominant flux (Bechtold et al., 2014). These models are more sensitive than the linear ones in the shallow groundwater zone—each centimeter of exposed peat corresponds to an additional annual release of 0.4-0.5 tons of CO_2 per hectare, with saturation occurring around 40 cm (Tiemeyer et al., 2020; Koch et al., 2023). These two modelling philosophies, their contrasting sensitivities across groundwater levels, and the published slopes used in this study are illustrated in Fig. 1 and summarised in Table 2 in the Discussion.

The causal diagram (Fig. 2) illustrates the interconnected controls of climate drivers, hydrology, and soil properties on peat oxidation in Dutch peatlands. Groundwater level regulates air-filled pore space and oxygen availability, which together shape microbial degradation rates (Kechavarzi et al., 2010; Song et al., 2021). Clay layers and intrinsic soil characteristics further modulate water retention and oxygen diffusion, while climate influences both soil temperature and moisture conditions. These interacting pathways determine how much soil organic matter becomes exposed and prone to oxidation, emphasizing that peat

https://doi.org/10.5194/egusphere-2026-3151
Preprint. Discussion started: 24 June 2026
© Author(s) 2026. CC BY 4.0 License.

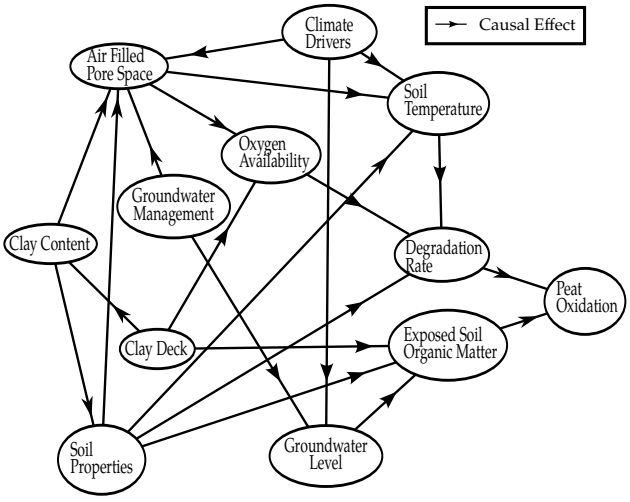

Fig. 2. Conceptual overview of the interacting controls on peat oxidation in Dutch peat soils, highlighting how climate drivers, groundwater level, soil temperature, clay layers, and air-filled pore space jointly regulate oxygen availability, exposed organic matter, and degradation rates.

degradation emerges from coupled feedbacks within the soil–hydrology–climate system rather than from any single controlling factor.

This complexity makes it inherently difficult to formulate a general ERF, especially because the annual groundwater level captures only a small part of the processes regulating peat oxidation. Peat decomposition responds to a suite of fast-changing biophysical conditions that groundwater metrics alone cannot fully represent. Microbial communities exhibit narrow moisture and temperature optima, and decomposition rates decline rapidly under drought, waterlogging, or thermal extremes (Preston et al., 2012; Song et al., 2021). Oxygen availability also varies over short time scales: diffusion constraints strongly limit aeration at depth, yet deep peat may become oxygenated during dry periods when cracking provides preferential pathways (Gebhardt et al., 2009). In addition, soil physical properties such as bulk density, porosity, hydraulic conductivity, and thermal inertia vary with peat type, moisture content, and degree of degradation, and differ markedly between compacted agricultural topsoil and deeper, less disturbed peat layers (Chan and van den Akker, 2022; Tolunay et al., 2024). These rapidly fluctuating biophysical controls are difficult to incorporate into ERFs, which necessarily aggregate them into annual or seasonal groundwater metrics. As a result, ERFs inevitably smooth over much of the temporal variability and spatial heterogeneity that shape CO_2 emissions, contributing to the observed non-linearity and site-specificity in groundwater–carbon relationships.

In individual studies, the impact on net carbon emissions can seem absent, for example, Veenendaal et al. (2007) and Schrier-Uijl et al. (2010) show similar annual emissions of about 15 $\mathrm{t_{CO_2}\ ha^{-1}\ yr^{-1}}$for both a deeply drained (water table down to -60 cm) and a shallowly drained peat meadow (water table down to -30 cm). Also, Weideveld et al. (2021), studying a range of peat meadows with and without subsurface infiltration measures, were unable to show an effect on CO_2 emission mitigation.

https://doi.org/10.5194/egusphere-2026-3151
Preprint. Discussion started: 24 June 2026
© Author(s) 2026. CC BY 4.0 License.

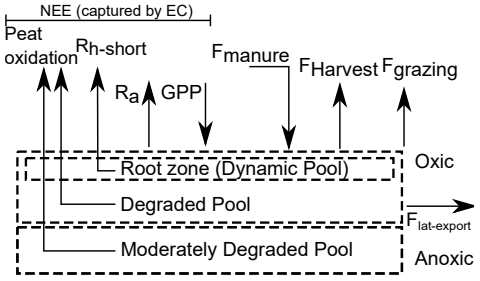

Fig. 3. Conceptual diagram of carbon fluxes and soil organic-matter pools in Dutch peat meadows. NEE measured by eddy-covariance integrates plant-driven fluxes (gross primary production (GPP), autotrophic respiration (R_a), short-term microbial respiration, and long-term peat oxidation from deeper degraded pools. Management practices add and remove carbon via manure application, harvest, and grazing, while hydrological control introduces lateral carbon export through pumped drainage water. The soil profile is divided into an oxic root zone overlying degraded and moderately degraded peat pools that transition into anoxic conditions, highlighting the hydrological regulation of peat decomposition and CO_2 emissions.

In quantifying the CO_2 emissions, the longer-term budgets (one year and longer) are considered the most relevant for reporting and assessing mitigation potential, because the emissions vary strongly over seasons and because management-related carbon transfers (export of harvest, grazing, and import of manure) is usually quantified annually only. A common approach is to measure Net Ecosystem Exchange (NEE) year-round and then correct for the imports and exports, yielding the so-called Net Ecosystem Carbon Balance (NECB), describing how much CO_2 leaves the system yearly:

$$\mathrm{NECB} = \mathrm{NEE}_{\mathrm{CO_2}} + F_{\mathrm{Harvest}} + \mathrm{F_{lat\text{-}export}} - \mathrm{F_{manure}} + \mathrm{F_{grazing}} - F_{\mathrm{lat\text{-}import}} \quad (1)$$

Note that this NECB does not account for CH_4, CO, or volatile organic carbon emissions. Lateral carbon fluxes — both exports (dissolved organic carbon in pumped drainage water) and imports (dissolved organic carbon in infiltrated ditch water) — were only estimated at the fully inundated paludiculture sites (Ankeveen, Zegveld) and are set to zero elsewhere. Harvest and manure data were available as single-value annual estimates without uncertainty ranges. CH_4 carbon losses are minor in the predominantly drained systems studied (Tiemeyer et al., 2016) and are reported in a companion paper (Buzacott et al., 2024). Conversion coefficients and methodology for harvest and manure terms are detailed in Appendix F.

As the main interest is in the emissions from degrading peat, an approach is needed to distinguish these emissions from those from the degradation of recently assimilated or imported organic matter. This is a non-trivial problem fraught with conceptual issues. For pastures, if they can be assumed not to accumulate new carbon on an annual basis, the NECB would equal the emissions from peat degradation. This follows because harvest, grazing, and manure terms are measured independently at parcel scale and included in NECB via Eq. 1; under the no-accumulation assumption, the net sum of all these terms equals the long-term peat carbon loss. However, the humic and litter layer underneath the grass may well vary from year to year as a result from varying weather conditions, diseases or disturbance by management, mice or insect herbivory (Shao et al., 2015; Hoover and Rogers, 2016). The exact export or import from grazing cattle ($\mathrm{F_{grazing}}$) is hard to assess and to interpret. The addition

https://doi.org/10.5194/egusphere-2026-3151
Preprint. Discussion started: 24 June 2026
© Author(s) 2026. CC BY 4.0 License.

of manure (F_{manure}) might imply the addition of carbon to the system but in a completely different form than peat or humus. Compensating for manure addition could erroneously reduce estimates of peat oxidation where relatively slowly decomposing peat may have been compensated for by rapidly decomposing manure carbon, and it would depend on the turnover time of the manure whether this affects annual NECB. In natural wetlands and paludiculture systems that accumulate organic material, quantifying the underlying peat degradation seems to be highly challenging at the field scale.

Throughout this paper, 'CO_2 emissions' refers to NECB when annual carbon budgets are discussed, and to NEE_{CO_2} when describing sub-annual or directly EC-measured fluxes; the relationship between these quantities is illustrated in Fig. 3.

This paper focuses on the CO_2 exchange (NEE and NECB) at field scale. We present an overview of the first years of data across all measurement sites on peat soils, stretching from deeply drained dairy fields to semi-natural reed lands and a shallow lake. Methane exchange, almost in every case measured alongside the CO_2 fluxes, has been covered in a similar way by a companion paper (Buzacott et al., 2024). First assessments of (annual) GHG global warming potentials will be given in a subsequent joint analysis. This paper addresses the following questions:

1. What are the magnitude and temporal dynamics of net ecosystem CO_2 exchange (NEE) in a range of peat–based pastures, wet and dry crops, and (semi-)natural vegetations? We expect ecosystem respiration to be high compared to other ecosystems and expect all managed ecosystems to be net emitters of CO_2.

2. How large are annual carbon budgets (NECB) and what are the uncertainties associated with gap filling, interpolating fragmentary datasets, and corrections for harvest, grazing and manure application? Can we detect differences between the different land-use types (pasture, paludiculture, natural wetland, open water)? We expect lower net CO_2 losses (lower NECB) in paludiculture and wetland sites, reflecting higher plant uptake and reduced peat oxidation, and sustained winter uptake in evergreen pastures.

3. How do CO_2 emissions (NECB) depend on the groundwater table dynamics, temperature and site characteristics? We expect that emissions will increase with average groundwater depth; however, it is unclear whether this relationship is linear or levelling off at a certain depth.

4. Can we detect effects of the groundwater management on net CO_2 emissions? We expect lower emissions (lower ecosystem respiration) in locations where groundwater is kept high throughout the year, but also expect that some management measures are more effective than others.

5. How do the ERFs and groundwater–CO_2 relationships derived from our dataset compare with those reported in existing studies? We evaluate whether the magnitude, variability, and groundwater sensitivity of ERFs estimated from Dutch peatlands are consistent with previously published values, and examine where and why deviations occur as a function of land use, management intensity, clay cover, and groundwater control.

The eddy covariance (EC) monitoring network, including detailed documentation of data processing and harmonization, is described in a companion data paper currently in preparation. The machine-learning modelling framework is presented in a separate methodological manuscript, also in preparation.

https://doi.org/10.5194/egusphere-2026-3151
Preprint. Discussion started: 24 June 2026
© Author(s) 2026. CC BY 4.0 License.

2 Methodology

2.1 Sites, treatments and classification

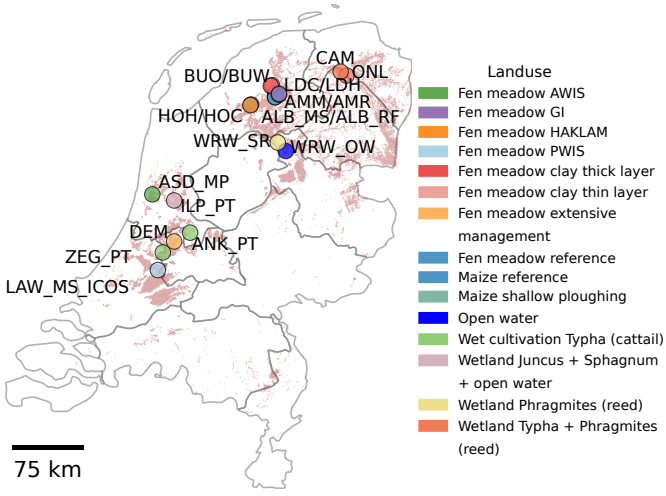

Fig. 4. Locations of the study sites across the Netherlands overlaid on the national peat map. Coloured symbols indicate the different land-use categories represented in the dataset, including fen meadows, maize systems, wet cultivation (reed/typha) or restored wetlands. Site codes correspond to individual eddy-covariance towers or paired management treatments. A more extensive description linking sites to their code is provived in Appendix A

Greenhouse gas emissions were measured across 20 Dutch peatlands (Fig. 4). The sites varied in vegetation (grassland, maize, *Typha*/*Phragmites* wetlands), land use (managed and natural), mitigation strategy, and soil type (pure peat or clay-covered peat). Site descriptions and classifications are provided in Appendix A. Ten of these measuring sites, the fluxes were only measured intermittently using a mobile eddy covariance setup, which is described in more detail below.

2.2 Eddy covariance measurements

Eddy covariance (EC) relies on fast-response (typically 10 Hz) measurements of vertical air movement (w) and concentrations (c) of the atmospheric constituents of interest as they advect from the upwind area to the sensors. The covariance of w and c essentially represents the vertical transport, but several more technical corrections and data filters are required. At all measurement locations, a similar measuring system was employed consisting of; a 3-D sonic anemometer (Gill Windmaster or R3, Metek uSonic-3 Cage MP), open-path, fast-response digital CO_2 and H_2Oanalyser (Li-Cor 7500DS or 7500RS), and (in most locations) an open-path fast-response CH_4analyser (Li-Cor 7700). At one site (LAW_MS) a closed-path gas analyser (Li-Cor 7200RS) was used, including a 15 lpm pump unit and a heated inlet tube (Li-Cor). The closed-path analyser at LAW_MS is not suitable for H_2O flux measurements due to time-lag uncertainty and spectral response limitations of the inlet system; H_2O fluxes at this site were therefore not used.

https://doi.org/10.5194/egusphere-2026-3151
Preprint. Discussion started: 24 June 2026
© Author(s) 2026. CC BY 4.0 License.

The equipment was mounted on top of telescopic masts and arranged side-by-side, perpendicular to the prevailing southwest winds and with 20-40 cm horizontal separation between the respective measuring paths (Fig. D1). Measuring height ranged between 1.5 and 6 m, and was tuned to optimise minimum height above the surface and the coverage of the typical footprint over the areas of interest, which are typically fields of only a few hectares and length scales of 100-200 m. All signals were acquired, stored and pre-processed by a Li-Cor Smartflux-3 or -2 unit and transmitted to a central data storage server every half hour via mobile internet connections.

At each site, meteorological measurements were also taken, including temperature, relative humidity, air pressure, wind direction and velocity, precipitation, incoming and reflected shortwave and longwave radiation, photosynthetically active radiation, and near-infrared radiation (Table E1). Soil variables were collected as well, including groundwater level at one or more locations, multi-depth soil moisture content and soil temperature, and ground heat flux. In most cases, several other observations were performed as the sites are part of the Netherlands Research Programme on Greenhouse Gas Dynamics in Peatlands and Organic Soils (NOBV) monitoring network. Grass or vegetation height, biomass, harvest, grazing and manuring in the main footprint direction were monitored over time in variable degrees of detail and frequency, to some extent limiting the analysis of annual carbon budgets.

To increase spatial coverage and include a broader range of peatland conditions, several locations were monitored using mobile eddy covariance towers. These compact systems were periodically relocated between predefined site pairs. Within each pair, the sites shared the same continuous meteorological measurements while the EC system rotated between them. This approach allowed more peatland types to be covered with limited equipment, but it created multi-week gaps in EC observations at each site, making robust gapfilling essential and reliant on the uninterrupted meteorological data.

2.2.1 Data Processing

Turbulent fluxes were calculated using the covariance of vertical wind speed and respective scalars of interest using EddyPro (v7.0.9, LI-COR Biosciences). Double coordinate rotation was used for tilt correction, block averaging for detrending, covariance maximisation for time lag detection, compensation for density fluctuations (Webb et al., 1980); fully analytic spectral corrections for the high frequency range (Moncrieff et al., 1997) fully analytic spectral corrections for the low frequency range (Moncrieff et al., 2004). The NEE for each scalar of interest was estimated by adding the single point storage estimate (using concentrations only at measurement height) to the turbulent flux (Aubinet et al., 2012). Although CO_2 concentrations do increase much during calm and warm nights (up to over 800 ppm – not shown here), the difference between surface and measurement height is limited to 6 m and generally only 2-3 m (see Appendix A). Therefore, we can assume that the additional CO_2 storage between surface and measurement height (equal to integrated concentration change over time times measurement height) caused by strong concentration gradients is small.

The EddyPro output was postprocessed using a series of filters. Flux data outside physically realistic bounds were excluded from the analysis; specifically, observations with $F_{CO_2} \notin [-50,\ 50]\ \mu\mathrm{mol\,mol}^{-1}$ were removed prior to further processing. Data was marked as missing if it had a quality flag of 2 (rejected) as determined by the (Foken et al., 2004) flag system, where 0 = excellent, 1 = acceptable, and 2 = rejected. The LI-COR CO_2 and CH_4 gas analysers have internal received signal strength

https://doi.org/10.5194/egusphere-2026-3151
Preprint. Discussion started: 24 June 2026
© Author(s) 2026. CC BY 4.0 License.

indicators (RSSI) and an RSSI threshold of 70 was used for CO_2 and 10 for CH_4. The latter threshold of 10 is used as it usually indicates that the mirrors were dirty and/or objects were obstructing the sample path (McDermitt et al., 2010). All hard flags defined by Vickers and Mahrt (1997) were applied, which screen the raw data for spikes, amplitude resolution, drop-outs, absolute limits, skewness and kurtosis, discontinuities, time lags, angle of attack, and steadiness of the horizontal wind. Timesteps where precipitation was recorded by the weather station were also deemed invalid. At some sites, wind direction filters were applied to exclude fluxes from unwanted areas, such as areas with different vegetation or built-up areas. The footprint was calculated with the two-dimensional parameterisation of Kljun et al. (2015), data were filtered out if less than 50% of the footprint strength was within a predefined area of interest. Periods at night with stable conditions, as indicated by the friction velocity ($u_\star$), were removed using a single, non-seasonal $u_\star$ threshold per site, determined with the moving point test (Papale et al., 2006). The meteorological data was filtered when exceeding a realistic threshold, or when any issues with the equipment were detected.

Missing NEE data were initially gapfilled using the marginal distributed sampling (MDS) algorithm (Reichstein et al., 2005). The algorithm uses a look-up table approach and fills missing flux data with the value of the average flux under similar global radiation, temperature, and VPD conditions. MDS was chosen for its simplicity and its established performance for filling short gaps of a few days to a few weeks (Moffat et al., 2007). Gaps greater than 60 days in length and gaps resulting from the mobile measuring strategy were not filled with the MDS algorithm; beyond this threshold, conditions at the time of the gap are too far removed from those of available look-up entries to yield reliable estimates, and the ML model described below is used instead. Only quality-controlled raw measured fluxes were used as targets for ML training and evaluation; MDS-filled values were excluded from both sets. Missing meteorological data was filled with data from nearby NOBV stations and KNMI (Dutch meteorological institute) stations.

Determination of the $u_\star$ threshold and gapfilling using the MDS method were performed using the R package REddyProc (Wutzler et al., 2018). Flux partitioning into ecosystem respiration (R_{eco}) and gross primary production (GPP) was also performed using the night-time partitioning method in REddyProc (Reichstein et al., 2005), but partitioned fluxes are not analysed in this paper.

2.3 Gapfilling, Additional Features, Engineering and Data Assembling

We derived several additional features from the vertical soil moisture and temperature profiles measured by the Sentek soil probes (Table 1). The total profile thickness L and the depth-weighted mean temperature $\hat{T}$ were computed from the layer thicknesses Δz_i and layer temperatures T_i recorded by the probes. Air filled pore space (AFPS) was defined as the vertical sum of $(\theta_{sat} - \theta_i)$ across layers, scaled by Δz_i, where θ_{sat} is a proxy for the true saturated volumetric water content, estimated as the site- and depth-specific maximum value recorded by the Sentek probe using the factory calibration, under the assumption that full saturation is reached each winter. No additional peat-specific correction was applied; θ_{sat} and the resulting AFPS should therefore be interpreted as relative indicators of wetness state rather than absolute volumetric quantities and θ_i the Sentek-measured volumetric water content in each depth. From these quantities, we derived an AFPS-weighted mean temperature T_{AFPS}, representing the thermal conditions in the unsaturated depth, and a complementary mean temperature T_{AFPS^c} for the

https://doi.org/10.5194/egusphere-2026-3151
Preprint. Discussion started: 24 June 2026
© Author(s) 2026. CC BY 4.0 License.

Table 1. Depth-aggregated features derived from soil moisture and temperature profiles measured using SENTEK Probe, see E1

Variable	Equation	Interpretation
L	$\sum_{i=1}^{N} \Delta z_i$	Depthof the soil profile, where SENTEK probe is used
$\hat{T}$	$\hat{T} = \frac{\sum_{i=1}^{N} T_i \Delta z_i}{L}$	Mean soil temperature along the profile
AFPS	$\sum_{i=1}^{N} (\theta_{\text{sat}} - \theta_i) \Delta z_i$	Air-filled pore space across the profile
T_{AFPS}	$\frac{\sum_{i=1}^{N} (\theta_{\text{sat}} - \theta_i) T_i \Delta z_i}{\text{AFPS}}$	Temperature weighted by air-filled pore space, proxy of the temperature of oxic zone of the profile
T_{AFPS^c}	$\frac{\theta_{\text{sat}} L \hat{T} - \text{AFPS}\, T_{\text{AFPS}}}{\theta_{\text{sat}} L - \text{AFPS}}$	Mean temperature of the complementary (water-filled) pore volume, proxy of saturated zone temperature

saturated part of the profile. These engineered features were included as covariates in the machine-learning models. It should be noted that the Sentek probes use a factory calibration developed for sandy mineral soils; the moisture content values derived for peat are therefore not absolute volumetric water contents but relative proxies for the wetness state of the profile. Accordingly, AFPS is used here as a relative indicator of unsaturated pore volume rather than as a calibrated absolute measure, and its role is limited to feature engineering for the ML gap-filling model.

We combined multiple datasets, including eddy covariance fluxes, meteorological variables, groundwater levels, soil and land-surface parameters, and optical remote-sensing products, following the workflow illustrated in Fig. 5. Each dataset was first filtered for data quality and screened for outliers or inconsistencies. After filtering, all data streams were temporally aligned and merged into a single master time series (Fig. 5a). Basic meteorological and site-level variables were used to construct the predictor set for flux gapfilling. Remote-sensing inputs (PlanetScope imagery and PlanetScope Moisture Products) were processed separately and subsequently added to the combined dataset.

For each site, the cleaned meteorological, soil, hydrological, and remote-sensing variables were used as covariates in the XGBoost (Chen and Guestrin, 2016) machine-learning gapfilling model (Fig. 5b). Model training employed a leave-one-group-out cross-validation strategy (LOGO-CV), where groups were defined as consecutive three-week blocks matching the rotation interval of the mobile eddy covariance setup. This ensured that withheld test periods were temporally separated from

https://doi.org/10.5194/egusphere-2026-3151
Preprint. Discussion started: 24 June 2026
© Author(s) 2026. CC BY 4.0 License.

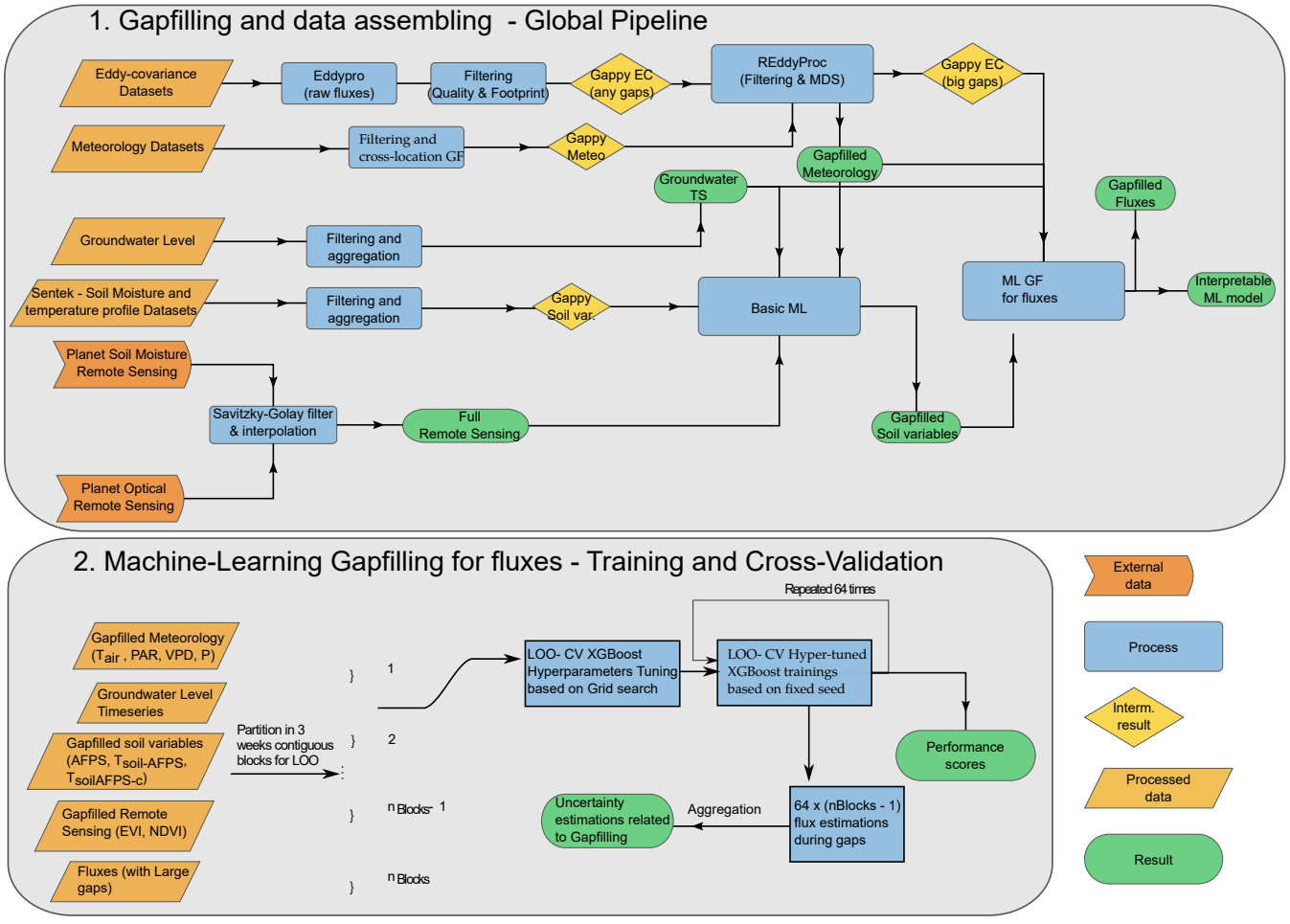

Fig. 5. (1) Global pipeline for assembling all input data streams (eddy-covariance, meteorology, groundwater level, sentek probe data, and remote-sensing products). Each dataset is filtered, quality-checked, and temporally aligned before being merged into a unified time series for modelling. Short gaps (<60 days) are first filled using the MDS algorithm; only quality-controlled measured (raw) fluxes are used as ML training targets — MDS-filled values are not. (2) Machine-learning gapfilling workflow for fluxes, including construction of predictor matrices, leave-one-group-out cross-validation (LOGO-CV with 3-week blocks), hyperparameter tuning, and aggregation of predictions into continuous flux time series.

https://doi.org/10.5194/egusphere-2026-3151
Preprint. Discussion started: 24 June 2026
© Author(s) 2026. CC BY 4.0 License.

training data by at least one full rotation cycle, reducing information leakage from adjacent time steps. While this blocking scheme is more realistic than random hold-out for time series data, residual seasonal autocorrelation within years means that cross-validation scores may still slightly overestimate predictive performance in practice. Hyperparameters were optimised separately within each training fold. Predictions from all folds were aggregated to produce continuous flux time series, while model performance was evaluated using the withheld data in each fold. Gap-filling uncertainty was quantified from two sources: epistemic uncertainty, estimated as the standard deviation across 64 repeated model runs with different random seeds; and aleatoric uncertainty, derived from the residuals of the leave-one-out cross-validation, reflecting irreducible variability in the measured fluxes. Both components were propagated to annual budget uncertainty estimates.

Model performance was evaluated using joint distributions of measured and predicted NEE, with marginal density estimates and residual analysis (Fig. B1), acknowledging that uncertainty is typically highest during day–night transition periods. As with all tree-based models, XGBoost cannot extrapolate beyond the flux range observed during training; performance at extreme flux values during anomalous events should therefore be interpreted with caution.

2.4 Groundwater ERF-fitting and data aggregation

Annual budgets were calculated by aggregating fluxes and groundwater levels over complete calendar years, assuming winter to exhibit the lowest flux magnitudes. Groundwater levels were recorded by NOBV dipwells typically installed to a maximum depth of approximately 1–1.5 m below the surface; groundwater levels exceeding this range were recorded at the installation depth limit. Mean annual groundwater levels at deeply drained sites may therefore be slightly biased towards shallower values, which should be considered when interpreting ERF slopes at the deeper end of the groundwater range. Mean annual fluxes were related to mean annual groundwater levels using Reduced Major Axis (RMA) regression (Dumortier et al., 2021). RMA is preferred over Ordinary Least Squares (OLS) for three reasons: (1) both NECB and annual mean GWL carry substantial uncertainty (gap-filling error and temporal aggregation for NECB; measurement and spatial representativeness error for GWL), so the OLS assumption of an error-free predictor is violated; (2) using annual mean GWL as a proxy for the true instantaneous driver introduces additional representativeness error on the x-axis, which OLS would absorb as attenuation bias (slope dilution), systematically underestimating the true sensitivity; (3) the goal is to estimate a physical relationship between the two variables, not to minimise prediction error for new observations—the inferential target for which RMA is the appropriate estimator. The resulting ERF slopes are therefore comparable to those reported in Evans et al. (2021), who also applied RMA, and are not directly comparable to OLS-derived slopes from other studies. Analyses were conducted in Python using the pylr2 package (regress2 function), (Haentjens, 2018). Uncertainty bars were derived from the standard deviation of annual budgets obtained through LOOCV-based gap-filling. Aben et al. (2024) also applied Deming regression to their automated-chamber dataset (reported in their appendix), an approach analogous to RMA in that it accounts for uncertainty in both variables.

For the seasonal NEE trend analysis, each year was divided into three calendar seasons, and NEE data were aggregated as daily averages using only complete days.

https://doi.org/10.5194/egusphere-2026-3151
Preprint. Discussion started: 24 June 2026
© Author(s) 2026. CC BY 4.0 License.

3 Results

3.1 Seasonal patterns of net ecosystem exchange

Net ecosystem exchange (NEE) exhibits pronounced seasonal variation across land-use types (Fig. 6), reflecting differences in vegetation phenology, management intensity, and soil conditions (Jacobs et al., 2007; Falge et al., 2002). Negative NEE values indicate net CO_2 uptake.

Dairy pastures exhibit their strongest net CO_2 uptake in spring (AMJ), with uptake declining through summer. This pattern reflects early biomass development (grass growth) followed by mowing or grazing. Pastures with a clay layer over peat consistently show lower summer CO_2 emissions than those on bare or shallow peat at comparable drainage depths—a difference attributable to soil characteristics rather than management (Nijman et al., 2024).

Croplands and biomass-productive paludiculture systems, by contrast, reach peak CO_2 uptake in summer (JAS), reflecting later canopy closure and vegetation phenology. Despite this summer uptake, peat croplands remain the largest net CO_2 sources overall (Tiemeyer et al., 2016, 2020). Their delayed and shortened uptake period creates a narrow assimilation window that cannot offset high respiration rates and peat oxidation during the remainder of the year.

Wetlands display greater seasonal NEE variability, with several sites acting as seasonal CO_2 sinks and others as sources; several sites show substantial seasonal CO_2 uptake, though generally lower than biomass-productive paludiculture systems. *Sphagnum*-based paludiculture (ILP_PT) differs markedly from other paludicultures in Fig. 6. This site represents early-stage establishment, where *Sphagnum* cover remains incomplete and vegetation structure resembles *Juncus*-dominated or semi-natural grasslands. Consequently, its seasonal CO_2 uptake is comparable to extensive grasslands rather than biomass-productive paludiculture. NECB estimates for ILP_PT should therefore be interpreted with caution; the anomalous flux values at this site likely reflect its transitional vegetation state rather than a representative paludiculture carbon balance.

Across all land uses, net CO_2 emissions frequently persist into autumn (OND), highlighting continued ecosystem respiration and peat oxidation beyond the primary assimilation period—an asymmetry that shapes annual carbon balances (Falge et al., 2002; Schrier-Uijl et al., 2014). The modest differences observed between treatments do not capture short-term anthropogenic disturbances, such as mowing or manure application, which induce transient changes in NEE that are smoothed by the seasonal aggregation used here.

https://doi.org/10.5194/egusphere-2026-3151
Preprint. Discussion started: 24 June 2026
© Author(s) 2026. CC BY 4.0 License.

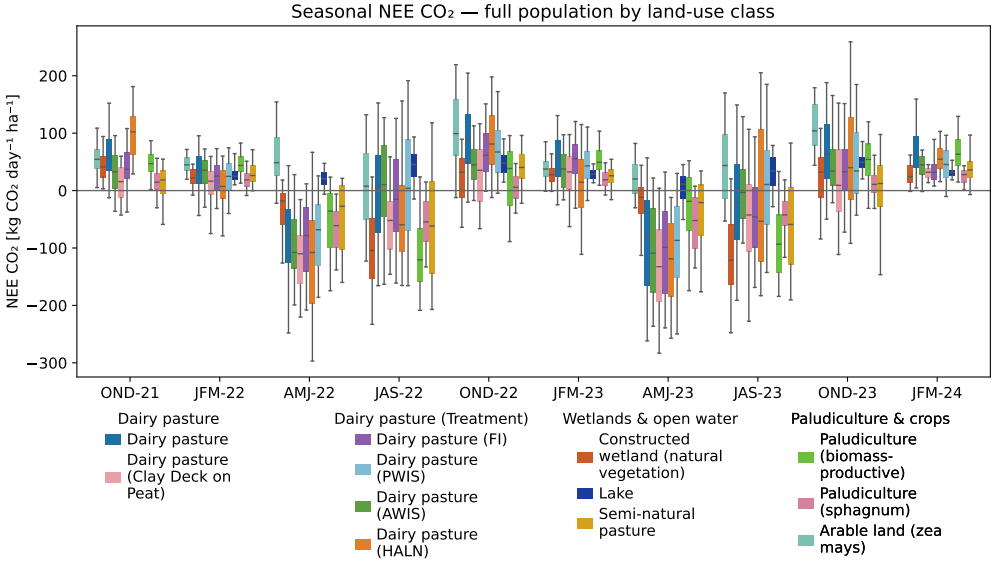

Fig. 6. Seasonal distributions of net ecosystem exchange (NEE) of CO_2 across land-use categories from OND-2021 to JFM-2024 (negative values indicate net CO_2 uptake). Dairy pastures show peak uptake in spring (AMJ), with lower summer emissions where a clay layer overlies peat, indicating reduced peat oxidation. Croplands and most paludiculture systems peak in summer (JAS), yet croplands on peat exhibit the largest net CO_2 emissions, as their uptake period starts late and ends early. Wetlands show variable but sometimes substantial uptake, while *Sphagnum*-based paludiculture is comparable to extensive grasslands. Across all land uses, net CO_2 emissions often persist into autumn (OND). Boxes represent inter-site variability within each category.

3.2 Relationship between NECB and groundwater level

NECB varied considerably across sites and years, showing only a weak relation , left panel). Although NECB increased with deeper groundwater, substantial scatter and low R^2 values indicate that surface-referenced groundwater depth provides limited explanatory power. The linear fit is applied here following standard practice in the field (Evans et al., 2021; Jurasinski et al., 2016); the wide scatter reflects genuine site-to-site variability rather than a failure of the linear approximation, which is not expected to capture all drivers of NECB at individual sites.

Sites with similar mean groundwater levels displayed markedly different NECB values, underscoring the influence of strong site-specific controls. Several pronounced deviations corresponded to sites underlain by a marine clay layer, a characteristic feature of Friesland peatlands that reduces the exposure of organic matter and limits oxygen availability (Nijman et al., 2024).

3.3 Influence of groundwater reference depth

Referencing groundwater level to the clay layer produced a clearer NECB relationship (Fig. 7, right panel). This analysis is restricted to the subset of sites where clay layer depth was known from soil profile descriptions; sites without a clay layer are represented only in the surface-referenced panel. For sites where the mean annual groundwater level was at or above the soil

https://doi.org/10.5194/egusphere-2026-3151
Preprint. Discussion started: 24 June 2026
© Author(s) 2026. CC BY 4.0 License.

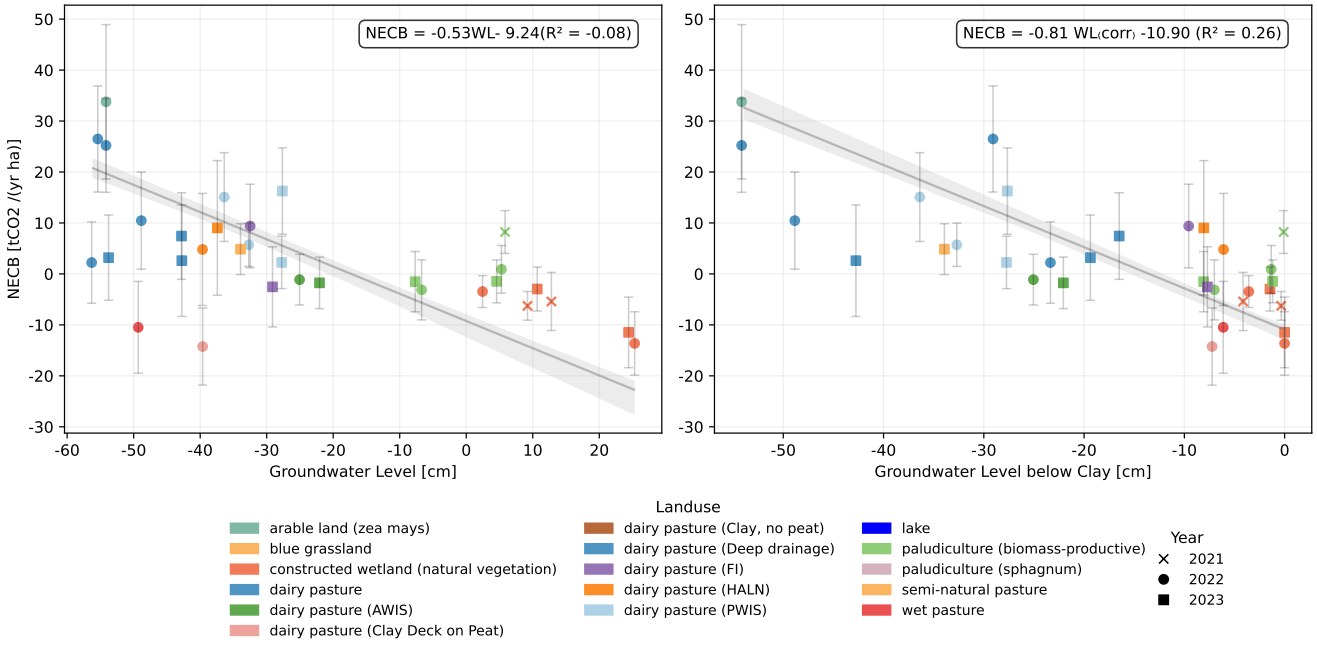

Fig. 7. NECB versus groundwater level across sites and years. Left panel: NECB plotted against mean annual groundwater level relative to the soil surface. Right panel: NECB plotted against mean annual groundwater level relative to the clay layer. Points represent site–year combinations coloured by land-use category. Error bars indicate uncertainty in annual NECB estimates. Solid lines show linear regressions with shaded 95 % confidence intervals.

surface (fully inundated conditions), the clay-referenced depth is set to zero, as the entire peat profile above the clay layer is saturated and no aerobic decomposition zone exists. NECB increased more consistently with depth below the clay layer, and explained variance exceeded that using a soil-surface reference. The clay layer thus serves as a more hydrologically and biogeochemically meaningful reference for peat carbon dynamics at these sites.

However, substantial variability persisted at similar clay-referenced depths, indicating that groundwater level alone does not determine annual NECB, and that the clay layer itself can vary considerably in organic matter content and associated biogeochemical properties (van den Akker et al., 2010).

3.4 Land-use and management effects on NECB

Across both representations, land-use categories occupied partially distinct regions in NECB–groundwater space (Fig. 7). Fen meadows, maize systems, and wet cultivation sites each showed broad NECB ranges, indicating that carbon balance reflects combined effects of hydrology, vegetation, management intensity, and site history beyond groundwater level alone (Jacobs et al., 2007; Evans et al., 2021).

https://doi.org/10.5194/egusphere-2026-3151
Preprint. Discussion started: 24 June 2026
© Author(s) 2026. CC BY 4.0 License.

3.5 Control–treatment comparisons

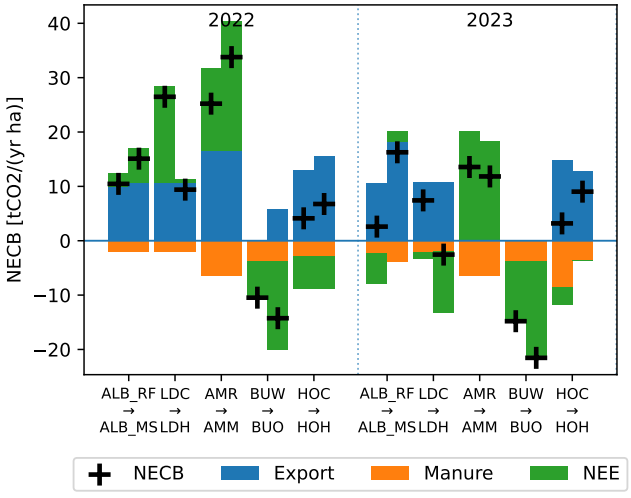

Fig. 8. NECB for paired control–treatment sites in 2022 and 2023. Stacked bars show the contributions of NEE, carbon export, and manure inputs to NECB, while black crosses indicate the resulting annual NECB. Positive values denote net carbon loss to the atmosphere. Site pairs are shown along the x-axis, with arrows indicating control–treatment comparisons; vertical dashed lines separate years. No carbon export term is reported for BUW in most years because this site is managed under extensive grazing by young cattle only, with no biomass harvest; the grazing contribution is captured by the $F_{grazing}$ term rather than an explicit export bar.

Paired control–treatment comparisons demonstrate that NECB differences cannot be attributed solely to groundwater conditions (Fig. 8; annual budget values in Table C1). Treatment effects often altered NECB primarily through changes in carbon export or import changes rather than NEE shifts, underscoring the importance of management interventions in modulating annual carbon balances (Weideveld et al., 2021; Aben et al., 2024).

3.6 Coupled responses of NECB to groundwater-level change

Interannual changes in annual NECB (ΔNECB) showed a moderate but consistent relationship with interannual changes in groundwater level (ΔWLEV) across sites and management types (Fig. 9). A linear fit indicated a negative association (ΔNECB $\approx -0.8\,\Delta$WLEV - 1.89), with ΔWLEV 37 % of the observed variability in ΔNECB ($R^2 = 0.37$). This relationship reflects a consistent sensitivity of NECB to hydrological change across sites.

Despite this overall trend, substantial scatter was observed, indicating pronounced inter-site variability in carbon balance responses to similar groundwater-level changes. Sites experiencing comparable increases in groundwater level did not systematically exhibit proportional NECB responses. In several cases, strong carbon losses occurred under relatively modest hydrological shifts, whereas other sites displayed limited NECB responses despite pronounced groundwater-level changes.

https://doi.org/10.5194/egusphere-2026-3151
Preprint. Discussion started: 24 June 2026
© Author(s) 2026. CC BY 4.0 License.

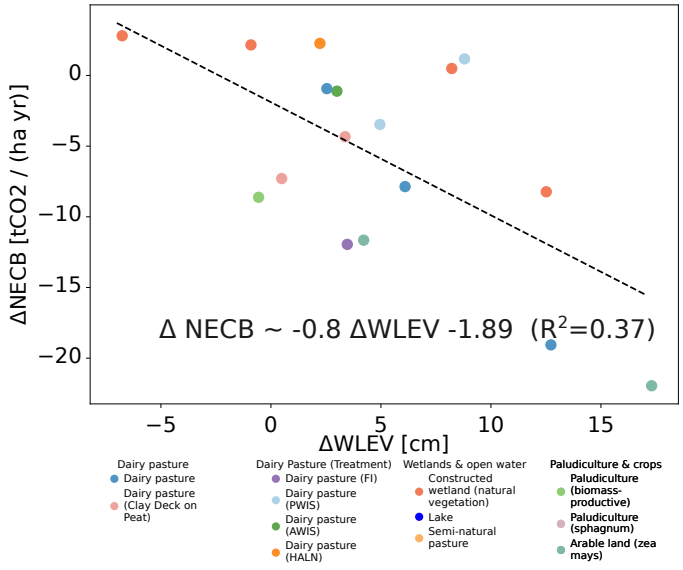

Fig. 9. Relationship between changes in annual net ecosystem carbon balance (ΔNECB) and changes in groundwater level (ΔWLEV) across managed peatland sites. Points represent site-level responses under different land-use and management categories (e.g. dairy pasture, wetlands, paludiculture, open water). Positive ΔNECB indicates increased net carbon loss to the atmosphere and negative ΔNECB indicates reduced net carbon loss; positive ΔWLEV corresponds to rising groundwater levels. The solid line shows the linear regression fit (ΔNECB $\approx -0.8\,\Delta\text{WLEV} - 1.89$, $R^2 = 0.37$).

Part of the observed scatter may also reflect methodological differences across sites, including uncertainties in the estimation of lateral carbon export fluxes.

Differences among land-use and management categories contributed to this variability. Managed dairy pastures, wetlands, and paludiculture systems occupied partially overlapping regions of the response space. Notably, more deeply drained systems, including croplands and reference dairy pastures, tended to exhibit higher NECB sensitivity to ΔWLEV than sites characterized by persistently high groundwater tables. This pattern contrasts with expectations from saturating response models (Tiemeyer et al., 2020; Koch et al., 2023) and indicates that NECB sensitivity remains elevated in systems operating farther from hydrological saturation.

4 Discussion

When comparing groundwater–carbon relationships across sites and studies, we focus on the NECB-slope rather than the NECB-intercept. The slope expresses the sensitivity of annual carbon balance to changes in groundwater level and we hypothesize that slopes are less influenced by site-specific baseline conditions (Evans et al., 2021; Tiemeyer et al., 2020). However, chemico-physical properties of the soil profile are likely to impact this relation. In contrast, intercepts integrate local effects of management and vegetation, which can vary substantially among sites. As a result, ERF slopes provide a more transferable

https://doi.org/10.5194/egusphere-2026-3151
Preprint. Discussion started: 24 June 2026
© Author(s) 2026. CC BY 4.0 License.

metric that reflects the physical control of groundwater level on the exposure of organic matter to aerobic decomposition, whereas intercepts primarily capture local context.

Table 2. Summary of published relationships between ERF slopes (ERF') and groundwater level (GWL) reported in previous studies on temperate peatlands. ERF slopes are reported for different groundwater depth intervals (-80–20 and -60–20 cm, where available), together with the groundwater level at which zero emissions are predicted and the groundwater depth associated with the maximum emission rate. Abbreviations used in the table are as follows: *Model* (Mod.)-L: linear, P: parabolic, G: Gompertz; *Monitoring* (Mon.)—EC: eddy covariance, MC: manual chambers, AC: automated chambers, ME: mesocosm experiments; *Region* (Reg.)-DE: Germany, UK: United Kingdom, NL: Netherlands, DK: Denmark, Global: a global dataset. An asterisk (*) indicates studies using summer groundwater level. (†) refers to the clay-referenced water level (-60–20 cm). (‡) Deming (orthogonal) regression fit from Aben et al. (2024); slope $= -15.13/100 \times 44/12 = -0.555\ \mathrm{t_{CO_2}\ ha^{-1}\ yr^{-1}\ m_{bgl}^{-1}}$, intercept $= -2.63 \times 44/12 = -9.64\ \mathrm{t_{CO_2}\ ha^{-1}\ yr^{-1}}$, zero-crossing at ≈ -17 cm bgl.

ERF'$_{[-80,20]/[-60,20]/max}$ [$\mathrm{t_{CO_2}\ ha^{-1}\ yr^{-1}\ cm^{-1}}$]	**GWL$_{0/max}$** [cm]	**Mod.**	**Mon.**	**Reg.**	**Ref.**
-0.41	0 / -	L	MC	DE	Jurasinski et al. (2016)
-0.49	-13 / -	L	EC	UK	Evans et al. (2021)
-0.34	-18 / -	L	EC	Global	Evans et al. (2021)
-0.31	0.6 / -	L	AC	NL	Aben et al. (2024)
-0.24	0.5 / -	L	AC	NL	Aben et al. (2024)*
-0.555	-17 / -	L	AC	NL	Aben et al. (2024)‡
-0.40/-0.50/-1.93	-9 / -16	G	MC	DE	Tiemeyer et al. (2020)
-0.40/-0.50/-2.09	- / -13	G	MC/ME	DK	Koch et al. (2023)
-0.82/-0.98/-2.24	- / -23	G	AC	NL	Nijman et al. (2024)
-0.46	-34 / -	L	EC	NL	van der Poel et al. (2025)
-0.53/-0.63/-0.83	- / 0	P	EC	NL	van der Poel et al. (2025)
-0.78/-0.80/-0.86	-176 / -24	G	EC	NL	van der Poel et al. (2025)
-0.54	-17 / -	L	EC	NL	This study
-0.81	-14 / -	L	EC	NL	This study†

The slopes of ERFs derived in this study (Fig. 7) are consistent with the range of previously published relationships linking annual CO_2 emissions to groundwater level (Table 2). We found the slopes to be sensitive to the choice of groundwater level reference.

When the groundwater level was referenced to the soil surface, we obtained an ERF slope of approximately -0.5 $\mathrm{t_{CO_2}\ ha^{-1}\ yr^{-1}\ cm^{-1}}$, which falls within the upper range of linear ERF formulations across comparable groundwater depth intervals. The Deming regression slope reported by Aben et al. (2024) ($-0.56\ \mathrm{t_{CO_2}\ ha^{-1}\ yr^{-1}\ m_{bgl}^{-1}}$, Table 2) is close to this estimate, providing independent support from an automated-chamber dataset.

Referencing the groundwater level to the base of the clay layer resulted in a steeper ERF slope of approximately -0.8 $\mathrm{t_{CO_2}\ ha^{-1}\ yr^{-1}\ cm^{-1}}$, which approaches the upper range of published ERF values and overlaps with slopes derived from non-linear models such as parabolic or Gompertz-type representations (Table 2). This increase in ERF magnitude aligns with the

https://doi.org/10.5194/egusphere-2026-3151
Preprint. Discussion started: 24 June 2026
© Author(s) 2026. CC BY 4.0 License.

improved correlation observed in the NECB–groundwater relationship when using a clay-referenced metric ($R^2 = 0.26$ vs. $R^2 = -0.08$ for the surface-referenced fit) (Fig. 7).

Despite this improvement, substantial scatter in annual NECB remains at similar clay-referenced groundwater depths, indicating that ERF slopes alone do not fully determine ecosystem-scale carbon balance. Variations in peat stratigraphy, presence or absence of clay layers, land use, management intensity, and interannual climatic variability likely contribute to the wide range of ERF values reported across studies and observed within this dataset (Evans et al., 2021; Tiemeyer et al., 2020; Aben et al., 2024).

Collectively, these findings support the use of ERF-based approaches as a first-order description of hydrological controls on annual CO_2 emissions, while emphasizing that their applicability and transferability depend on the definition of groundwater level and site-specific subsurface conditions. The automated-chamber dataset of Aben et al. (2024), collected at overlapping Dutch sites, yields comparable linear slopes (Table 2), providing independent support for the EC-derived sensitivities reported here; this paper focuses on the eddy-covariance perspective and does not attempt a direct site-level comparison between the two methods.

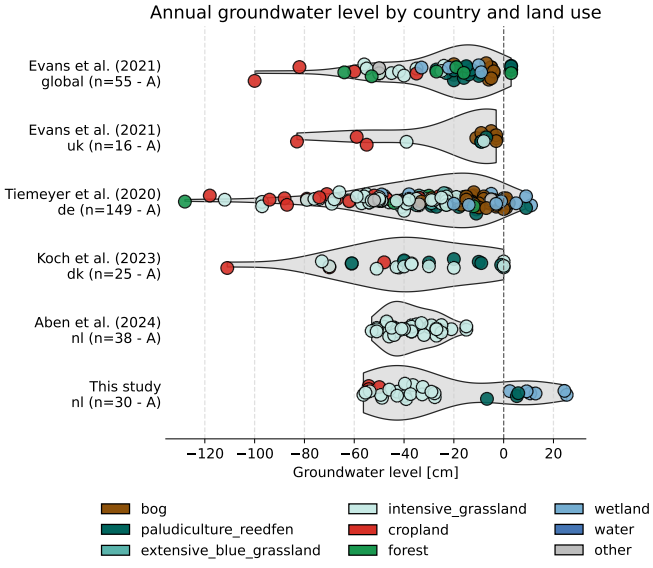

Fig. 10. Distribution of annual mean groundwater level by country and land-use category. The dataset now includes the automated-chamber measurements of Aben et al. (2024) (labelled 'aben') as an independent Dutch comparison group. Points represent site–year combinations coloured by land use, with shaded envelopes indicating the overall distribution within each country. Numbers in parentheses indicate sample size per dataset. The Kruskal–Wallis test indicated a significant overall difference among datasets ($H = 18.65$, $p = 0.0022$); post-hoc Dunn tests with Bonferroni correction showed significant differences only between the Aben dataset and the UK ($p = 0.011$) and between the Aben dataset and the global compilation ($p = 0.010$), consistent with the shallower groundwater levels in those datasets. All other pairwise comparisons were non-significant.

https://doi.org/10.5194/egusphere-2026-3151
Preprint. Discussion started: 24 June 2026
© Author(s) 2026. CC BY 4.0 License.

Although Dutch sites span groundwater level ranges broadly comparable to those observed elsewhere (Fig. 10), they are predominantly characterised by relatively shallow groundwater conditions, with few observations at very deep drainage depths, a pattern also observed for sites in the United Kingdom. By contrast, the automated-chamber dataset of Aben et al. (2024) covers a narrower groundwater range, concentrated around managed-grassland values (median -37.5 cm), because it does not include restored wetland or paludiculture sites. The Dutch EC dataset is therefore bimodal—deeply drained grasslands and croplands on one side, near-zero water-table wetlands and paludicultures on the other—whereas the Aben et al. (2024) dataset represents only the grassland segment of that distribution. As a result, many Dutch and UK sites are located within the groundwater depth range associated with the steepest part of published ERF curves reported in the literature (Table 2), where relatively small changes in groundwater level correspond to large changes in inferred CO_2 emissions. This positioning along the steepest part of published ERF curves provides a plausible explanation for the comparatively high ERF slopes observed in these regions, even in the absence of pronounced differences in overall groundwater-level distributions across countries.

In the Netherlands, this interpretation is strengthened by the strong representation of intensively managed peatlands with hydro-engineered water control, alongside a substantial number of restored wetlands and paludiculture sites in this study. Hydro-engineered measures such as controlled drainage and submerged drains are predominantly implemented in intensive grassland systems, where groundwater levels are actively regulated, while restored wetlands and paludiculture represent distinct land-use types characterised by persistently high water tables and different carbon and nutrient dynamics (Pijlman et al., 2020; Joosten, 2016). The coexistence of these contrasting but actively managed systems implies that Dutch ERF estimates integrate a wide range of land-use and management contexts rather than reflecting a single, homogeneous hydrological regime.

Differences among land-use classes in the NECB–groundwater relationship primarily reflect contrasts in the magnitude of NECB rather than differences in sensitivity to groundwater level (Fig. 11). Across land-use types, the slopes of the fitted relationships are broadly comparable, whereas intercepts and the range of NECB values differ substantially, indicating that baseline carbon balance conditions vary more strongly than the response to hydrological change.

Differences among countries become more apparent when considering annual NECB (Fig. 11), for which the distribution shows clearer separation than groundwater level alone. Despite broadly overlapping groundwater level distributions, NECB differs strongly among countries, indicating that ecosystem-scale carbon balance integrates additional controls beyond mean groundwater depth. In the Netherlands, NECB exhibits a wider spread than in other countries, consistent with the diversity of land-use types, management strategies, and monitoring method (EC) represented in the dataset. Importantly, this increased scatter does not correspond to a systematically higher NECB sensitivity to groundwater level (Fig. 7), but instead reflects the superposition of consistent groundwater control with strong land-use- and management-specific influences on carbon fluxes. Moreover, datasets from the Netherlands, the UK (Evans et al., 2021), and the global compilation (Evans et al., 2021) are dominated by eddy covariance measurements, whereas datasets from Denmark (Koch et al., 2023) and Germany (Tiemeyer et al., 2020) rely primarily on chamber-based or other small-scale approaches (Fig. 12), likely contributing to differences in observed variability and spatial aggregation scale. The Aben et al. (2024) dataset, restricted to managed grasslands, covers a narrower NECB range than the full Dutch EC dataset, consistent with its narrower groundwater range. Excluding wetland and paludiculture sites from the comparison, both the Dutch EC and Aben et al. (2024) datasets cluster in group A alongside the

https://doi.org/10.5194/egusphere-2026-3151
Preprint. Discussion started: 24 June 2026
© Author(s) 2026. CC BY 4.0 License.

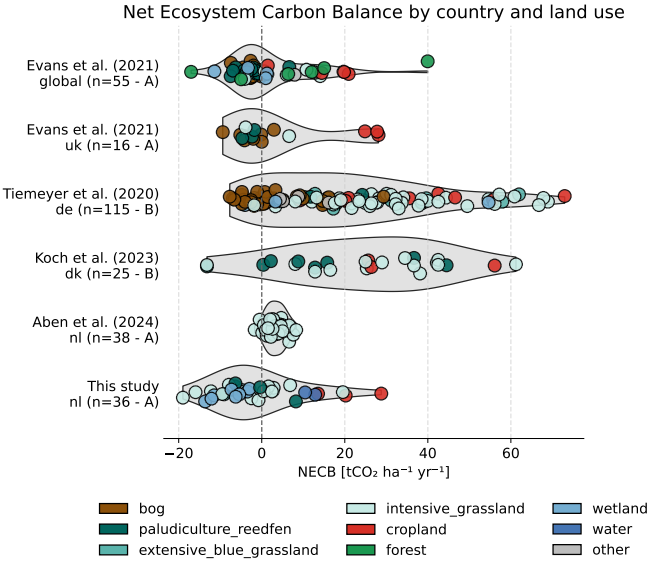

Fig. 11. Distribution of annual net ecosystem carbon balance (NECB) by country and land-use category. The dataset includes the automated-chamber measurements of Aben et al. (2024) (labelled 'aben') as an independent Dutch comparison group. Note that the Aben dataset covers only managed grasslands, so its NECB range is narrower than the full Dutch EC dataset, which additionally includes wetland and paludiculture sites. Points represent site–year combinations coloured by land use, with shaded envelopes indicating within-country distributions. Numbers in parentheses denote sample size per dataset; letters indicate groupings from post-hoc Dunn tests with Bonferroni correction. NECB differs strongly among datasets (Kruskal–Wallis, $H = 88.97$, $p < 10^{-16}$), despite overlapping groundwater level distributions.

UK and global compilations, and both differ significantly from Denmark and Germany (group B). This indicates that the higher NECB medians in the Danish and German datasets reflect genuine differences in drainage regime and site selection rather than measurement method.

Within the Netherlands dataset, fen meadow systems under business as usual management, mitigation-oriented systems with Passive Water Infiltration Systems (PWIS) and furrow infiltration occupy broadly comparable ranges of NECB and groundwater level. Croplands are generally more deeply drained and show larger NECB magnitudes. Active Water Infiltration System (AWIS) pastures tend to cluster at lower NECB values for similar groundwater levels, pointing to lower baseline carbon losses rather than a different groundwater–carbon relationship. Paludiculture systems, including *Typha*- and *Phragmites*-dominated sites, show slightly higher NECB values than restored wetlands despite consistently high groundwater tables. This likely reflects carbon export through biomass harvest in paludiculture systems (Pijlman et al., 2020; Joosten, 2016), although biomass removal can also occur in restored wetlands as part of good management practice. Overall, land use and management mainly affect the magnitude of NECB at a given groundwater level, while the general groundwater control appears comparable across systems. This pattern, observed across the diverse range of Dutch sites and land-use types, also holds when examining year-to-year variability within individual sites.

https://doi.org/10.5194/egusphere-2026-3151
Preprint. Discussion started: 24 June 2026
© Author(s) 2026. CC BY 4.0 License.

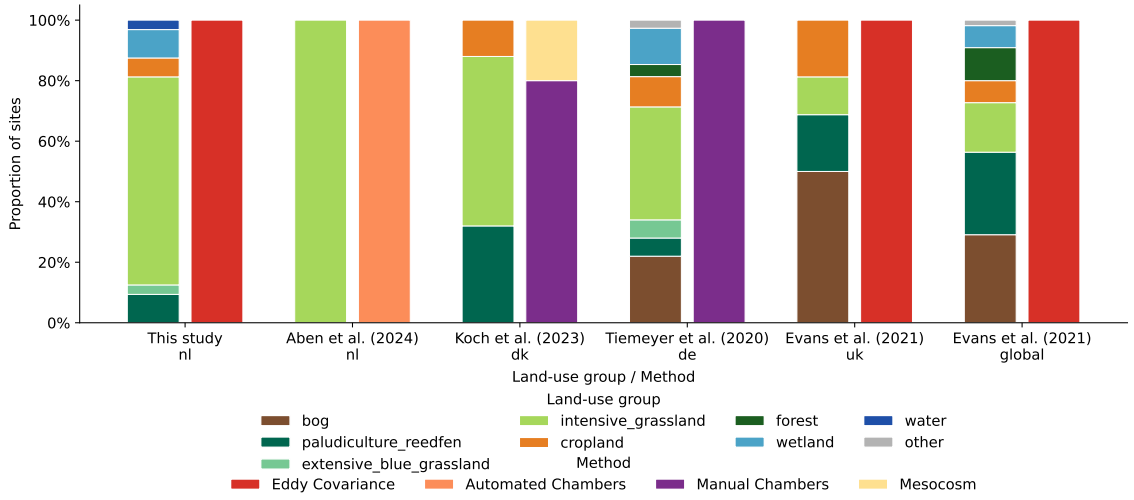

Fig. 12. Proportional distribution of sites across land-use categories by country and measurement method. Bars show the fraction of sites within each country belonging to a given land-use class, grouped by observation method (eddy covariance, manual chambers, mesocosms). Colours denote land-use categories. The *aben* column represents the automated-chamber dataset of Aben et al. (2024), composed entirely of managed grassland sites. The *global* column represents an independent global peatland dataset compiled using the same classification scheme, and is not an aggregate of the country-level subsets.

Shifting from cross-site spatial patterns to within-site temporal dynamics, interannual differences show a broadly consistent groundwater control on NECB. When expressed as year-to-year changes, ΔNECB scales linearly with ΔWLEV, yielding a slope close to -0.8 CO_2 / (ha yr) (Fig. 9). This slope reflects the aggregate of within-site year-to-year sensitivities (a slope-of-slopes) and is therefore conceptually distinct from a cross-site ERF slope, even where the numerical values are similar. The similarity between interannual and cross-site responses suggests that the inferred sensitivity of NECB to groundwater-level change is consistent across temporal and spatial scales (Evans et al., 2021; Kwon et al., 2022). Although interannual variability introduces additional scatter, the sensitivity of NECB to year-to-year groundwater variability is comparable in magnitude to the slope of the clay-referenced groundwater-level ERF, suggesting a consistent hydrological control across temporal scales.

These consistent sensitivities across temporal scales indicate that both paludiculture systems and deeply drained sites remain responsive to groundwater-level variability, however through different mechanisms. In paludiculture systems, NECB sensitivity likely reflects the dependence of biomass production and harvestable yield on water-level conditions (Pijlman et al., 2020; Joosten, 2016), so interannual fluctuations in groundwater level can directly affect carbon inputs and exports. In contrast, deeply drained systems, including croplands and conventional dairy pastures, remain sensitive to groundwater variability despite operating below the sensitivity range described by saturating models. Interannual fluctuations in groundwater level in these systems continue to influence aerobic decomposition and ecosystem carbon losses, consistent with the sensitivity inferred from year-to-year NECB changes. Together, these patterns suggest that NECB sensitivity to groundwater level is not restricted to a narrow hydrological regime, but can emerge through distinct mechanisms across management types.

https://doi.org/10.5194/egusphere-2026-3151
Preprint. Discussion started: 24 June 2026
© Author(s) 2026. CC BY 4.0 License.

Paludiculture sites represent a particular challenge for standardised carbon budget pipelines. Site managers and researchers with detailed knowledge of individual paludiculture sites have developed site-specific processing approaches tailored to the unique hydrological and ecological conditions of these systems, which may yield numerically different NECB estimates than those reported here. The present study deliberately applies a uniform pipeline across all 20 sites to ensure cross-site comparability; this choice prioritises consistency over site-specific precision, and some discrepancies with independently processed estimates of the same sites are therefore expected and do not necessarily reflect errors in either approach.

5 Conclusions and outlook

We integrated multi-year eddy covariance and chamber-based observations from a diverse array of managed peatland ecosystems to assess how groundwater level, reference depth, land use, and management influence annual net ecosystem carbon balance (NECB). Groundwater level consistently emerged as a determinant of carbon exchange across sites and years. However, its explanatory power depended on how hydrological depth was defined and on soil profile characteristics. Referencing groundwater to the soil surface resulted in weak and variable relationships with NECB. In contrast, referencing groundwater depth to the clay layer improved consistency across sites and produced steeper ERF slopes, however predictive power remains weak. These findings highlight the importance of accurately identifying air-exposed peat layers and the need for site-specific soil profile descriptions, which are often poorly captured by large-scale modelling. While detailed soil carbon stock and bulk density profiles were unavailable, spatially explicit information on the presence and thickness of the clay layer was available for Friesland. This provided a consistent stratigraphic reference that supports the use of clay-referenced groundwater depth as a meaningful hydrological metric.

Despite this improved relationship strength, NECB showed substantial variability even at similar clay-referenced groundwater depths. This variability reflects the combined effects of land use, vegetation phenology, management intensity, and carbon imports and exports, which are not captured by groundwater metrics alone. Control–treatment comparisons support this, showing that management interventions often altered NECB by changing biomass removal or organic matter inputs rather than solely by modifying net ecosystem exchange (NEE). In managed systems, groundwater management is closely coupled to aboveground practices, as water-table regulation influences grazing pressure, mowing frequency, fertilization intensity, and livestock stocking rates. Groundwater level affects NECB both directly, through peat oxidation, and indirectly, by shaping biomass production and carbon imports and exports. This tight coupling is a fundamental distinction from peatlands under non-productive land uses, such as bogs or semi-natural meadows, where hydrological variability primarily affects carbon exchange through biogeochemical and vegetation-mediated processes rather than coordinated management changes. Consequently, the pathways linking groundwater level to NECB differ substantially between intensively managed peatlands and systems where land use remains relatively decoupled from hydrological control.

Seasonal patterns of NEE provided additional insight into annual carbon outcomes. Dairy grasslands typically showed strong carbon uptake in spring, with assimilation declining in summer due to mowing and grazing. Croplands and biomass-productive paludiculture systems reached peak uptake later in the growing season, yet often remained net annual carbon sources because

https://doi.org/10.5194/egusphere-2026-3151
Preprint. Discussion started: 24 June 2026
© Author(s) 2026. CC BY 4.0 License.

of shorter uptake periods and sustained respiration. Across all land uses, net CO_2 emissions frequently extended into autumn, underscoring the importance of post-growing-season respiration and peat oxidation in shaping annual carbon balances.

The ERF slopes identified in this study align with the range of published groundwater–CO_2 relationships, with clay-referenced slopes approaching the upper limits of previous estimates. Many existing ERF formulations are strongly influenced by the intercept of the groundwater–carbon relationship, which integrates site-specific effects of peat properties, vegetation, and management history. Unlike slopes, which describe sensitivity to changes in groundwater level, intercepts depend on local baseline conditions and are difficult to transfer across sites or regions without additional site-specific information. Variations in NECB distributions across countries, despite broadly similar groundwater-level ranges, indicate that ecosystem-scale carbon balance emerges from the interaction of hydrological controls with region-specific land-use composition, management practices, and monitoring methodologies. In the Netherlands, for instance, the coexistence of intensively managed peatlands, engineered drainage systems, restored wetlands, and paludiculture leads to pronounced NECB variability that cannot be explained by groundwater depth alone.

Several limitations of the present analysis point toward priorities for future research. The approximately 2.5-year temporal coverage at many sites restricts inference on interannual variability and delayed ecosystem responses. Detailed soil carbon stock and bulk density data were unavailable for most sites. Unlike studies conducted under relatively homogeneous conditions using automated chambers, the pronounced heterogeneity observed at the parcel scale in this dataset justified excluding sparse or unrepresentative soil profile information. While soil properties are essential for linking fluxes to long-term carbon stocks, their inconsistent availability would likely have increased uncertainty rather than improved interpretability.

Future research should prioritize extending time series and leveraging harmonized datasets across the full EC NOBV network, while explicitly incorporating management descriptions to improve the robustness and transferability of groundwater–carbon relationships. Training ERF-based frameworks on larger and more diverse datasets will help constrain sensitivities across climates, peat types, and management regimes, enabling better resolution of non-linear responses under hydrological extremes. Integrating explicit management practices such as mowing, grazing, harvest, manure application, and hydrological engineering, together with subsurface stratigraphy and soil properties, is essential for developing mechanistic and policy-relevant carbon accounting.

Further progress will require closer integration of remote-sensing and footprint-based datasets. High-resolution optical and radar observations can provide spatially explicit information on vegetation dynamics, disturbance events, and surface moisture conditions, while footprint models offer a framework for linking flux measurements to heterogeneous source areas. Combining these spatial datasets with long-term flux observations will improve attribution of observed carbon exchanges and reduce uncertainty from spatial mismatches between measurements and ecosystem properties.

The ERF slope of approximately $-0.5\ \mathrm{t_{CO_2}\,ha^{-1}\,yr^{-1}\,m_{bgl}^{-1}}$implies that a 10 cm rise in annual mean groundwater level corresponds to a reduction of approximately 5 $\mathrm{t_{CO_2}\,ha^{-1}\,yr^{-1}}$, providing a practical order-of-magnitude benchmark for evaluating the climate mitigation potential of groundwater management interventions. At landscape scale, land use emerged as the primary driver of carbon balance: restored wetlands and paludiculture systems showed systematically lower net CO_2 emissions than drained managed grasslands, and the presence of a clay cap further reduced emissions independently of management.

https://doi.org/10.5194/egusphere-2026-3151
Preprint. Discussion started: 24 June 2026
© Author(s) 2026. CC BY 4.0 License.

From an applied perspective, groundwater-based ERFs are often presented as a practical way to upscale flux observations for regional carbon accounting, provided that groundwater data are widely available and hydrology is a key control on peatland emissions. However, the large variability observed at similar groundwater depths—driven by management, peat properties, vegetation, and biomass dynamics—demonstrates that groundwater is not the sole determinant of carbon exchange. As a result, ERFs primarily capture broad, large-scale trends and are useful for screening or benchmarking, but relying on them alone for local or parcel-scale emission estimates is risky. They cannot replace site-specific monitoring when accurate greenhouse gas assessments are required.

In summary, ERF-based approaches provide a valuable first-order framework for understanding hydrological controls on peatland carbon emissions and for translating existing observational data into actionable insights at regional and national scales. Their applicability depends on the choice of hydrological reference depth, subsurface conditions, and land-use management. The diversity of peat soils, management regimes, and biomass dynamics observed across sites shows that ERFs currently reflect large-scale patterns rather than locally precise carbon balances. Advancing peatland carbon assessments and supporting robust mitigation strategies and carbon accounting frameworks in managed peatland landscapes will require integrating long-term observations, globally calibrated relationships, explicit management descriptors, spatially resolved remote-sensing information, and sustained site-specific monitoring networks.

https://doi.org/10.5194/egusphere-2026-3151
Preprint. Discussion started: 24 June 2026
© Author(s) 2026. CC BY 4.0 License.

Appendix A: Site description

A Sites description

Table 1: Site description and instrumentation summary for all study locations. Land-use categories are harmonised across sites. Dairy pastures include different water-management regimes: **AWIS** (Active Water Infiltration System), **PWIS** (Passive Water Infiltration System), **BAS** (Business As Usual, conventional drainage management), and **HAKLAM** (*Hoger peil Als het Kan, Lager Als het Moet*), an adaptive water-level management strategy in which surface-water levels are raised during dry periods to limit peat oxidation and associated CO2 emissions, and temporarily lowered during wet conditions to maintain drainage capacity. Groundwater (GW) table values are expressed relative to the soil surface (negative values indicate groundwater below the surface). Where reported, summer and winter values represent seasonal means. Vegetation height refers to the dominant canopy. Tower height varied at some sites depending on vegetation height (*); in a few cases the mast height was adjusted during the measurement period (ˆ). Water-level ranges in parentheses indicate measurements from different plots within the same site (#).

Site name	Site ID	(Lon/Lat)	Tower height (m)	Land use	Soil type	Top clay layer thickness (cm)	Vegetation	Vegetation height (m)	GW table (cm-surface) Summer	GW table (cm-surface) Winter	Installation
Zegveld	ZEG_PT	(52.72,6.00)	3	Paludiculture (biomass-productive)	Peat	-	*T. latifolia*	0.1-2.5	4.3	8.8	Permanent
Ankeveen	ANK_PT	(52.25,5.10)	2.5-5*	Paludiculture (biomass-productive)	Sand, peat top	-	*T. latifolia, Carex spp, Juncus spp, T. angustifolia*	0.1-2.5	17.4 (-20.4)	6.5 (-7.1)#	Permanent
Assendelft	ASD_MP	(52.48,4.74)	2.5	Dairy pasture (AWIS)	Peat/clay top	30	*L. perenne*	0.15	-21.4	-2.80	Permanent
Ilperveld	ILP_PT	(52.44,4.95)	2.5	Paludiculture (sphagnum)	Peat, clay top	-	*Carex spp, Juncus spp*	0.5	-5.9	-1.0	Permanent
Weerribben	WRW_SR	(52.77,5.93)	2.5, 6ˆ	Constructed wetland (natural vegetation, peat excavation area)	Peat	-	*P. australis, Sphagnum spp, Typha spp*	0.1-2.5			Permanent
Duinigermeer	WRW_OW	(52.72,6.00)	2.5	Lake (peat excavation area)	Peat sludge	-		0.01			Permanent
Aldeboarn	ALB_MS	(53.05, 5.90)	1.5	Dairy pasture (PWIS)		30	*L. perenne*	0.15	-42.5	-7.2	Permanent
	ALB_RF	(53.05, 5.90)	1.5	Dairy pasture (BAU)		30	*L. perenne*	0.15	-78.4	-4.0	Permanent
	AMM	(53.03,5.90)	1.8-3.5*	Arable land (zea mays, intercropping)		-	*Z. mays*	0.1-2.5	-61.1		Mobile
	AMR	(53.03,5.90)	1.8-3.5*	Arable land (zea mays, BAS)		-	*Z. mays*	0.1-2.5	-68.1	-23.9	Mobile
De Burd	BUO	(53.10,5.87)	1.8	Dairy pasture (clay deck on peat)	Peat/clay top	45	*L. perenne*	0.15	-60.2	-11.1	Mobile
	BUW	(53.10,5.86)	1.8	Dairy pasture (clay deck on peat)	Peat/clay top	65	*L. perenne*	0.15			Mobile
Demmerik	DEM	(52.20,4.95)	6.8	Semi-natural pasture	Peat / decomposed top	-	*L. perenne*	0.15-0.3		-18.3	Permanent
Hommerts	HOC	(52.99, 5.68)	1.8	Dairy pasture (BAS)		35	*L. perenne*	0.15	-74.0	-24.2	Mobile
	HOH	(52.99, 5.67)	1.8	Dairy pasture (HALN)		45	*L. perenne*	0.15	-62.0	-17.5	Mobile
Langeweide	LAW_MS	(52.04,4.79)	6.6	Dairy pasture (PWIS)	Peat/clay top	-	*L. perenne*	0.15	-24.1		Permanent
	LAW_MOB	(52.04,4.79)	1.8,3.5,5.8		Peat/clay top	-	*L. perenne*	0.15			Mobile
Lytse Deelen	LDC	(53.05, 5.94)	1.8	Dairy pasture (BAS)		30	*L. perenne*	0.15	-73.0	-13.3	Mobile
	LDH	(53.05, 5.94)	1.8	Dairy pasture (FI)		30	*L. perenne*	0.15	-41.3	-2.8	Mobile
Onlanden	ONL	(53.18, 6.52)		Constructed wetland (natural vegetation)	Peat	15	*T. latifolia and P Australis*	2.0	9.1	-11.9	Mobile
Camphuys	CAM	(53.15, 6.58)	4.8-6.1	Constructed wetland (natural vegetation)	Peat/clay top	15	*S. erectum, G. maxima, P. australis*	2.0	28.5	14.5	Mobile

https://doi.org/10.5194/egusphere-2026-3151
Preprint. Discussion started: 24 June 2026
© Author(s) 2026. CC BY 4.0 License.

Appendix B: Cross-validation - results

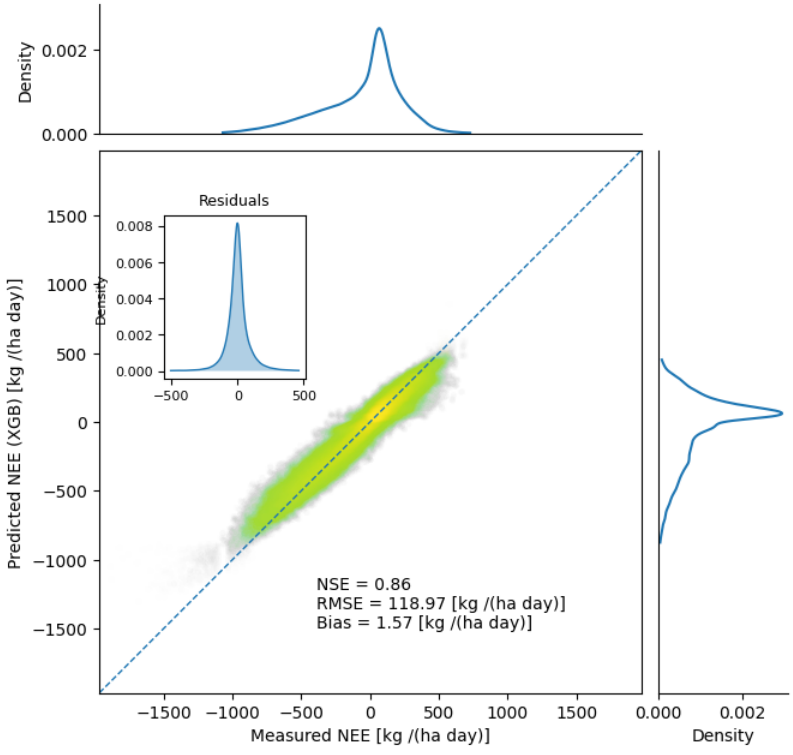

Fig. B1. Comparison between measured and predicted net ecosystem exchange (NEE). The central panel shows predicted versus measured NEE, with the dashed line indicating the 1:1 relationship. Marginal kernel density estimates illustrate the distribution of fluxes, and the inset shows the residual distribution. Performance metrics (NSE, RMSE, and bias) are reported in the panel. Largest discrepancies are mainly associated with day–night transition periods, while saturation and overall performance remain acceptable for large flux magnitudes.

On Figure B1, this joint distribution highlights that most deviations between measured and modelled NEE occur around the day–night transition. These periods are known to be the most challenging for eddy-covariance measurements and gap-filling models, due to rapidly changing turbulence regimes, low friction velocity, and sign reversals in fluxes (Vekuri et al., 2025). In contrast, the model shows acceptable saturation behaviour for large positive and negative fluxes, where turbulent conditions are generally well developed and the signal-to-noise ratio is higher. As a result, residuals remain comparatively small at high flux magnitudes, while increased scatter is concentrated around near-zero fluxes associated with dawn and dusk.

Figure B2 presents the distribution of model residuals (predicted − observed NEE) as a function of measured NEE, using equal-width bins along the measured flux axis. The upper panel shows the marginal distribution of measured NEE, highlighting the strong concentration of observations around near-zero fluxes, while large uptake and release events occur comparatively rarely.

https://doi.org/10.5194/egusphere-2026-3151
Preprint. Discussion started: 24 June 2026
© Author(s) 2026. CC BY 4.0 License.

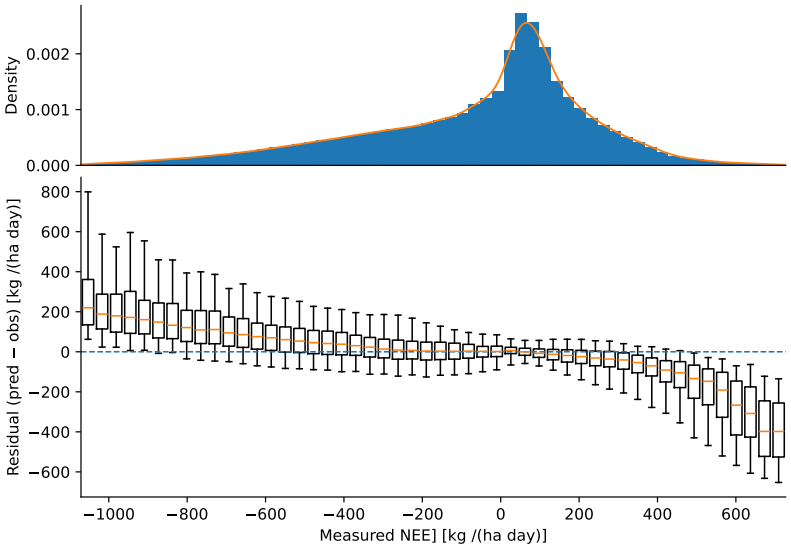

Fig. B2. Residual diagnostics of the NEE gap-filling model as a function of measured flux. The upper panel shows the distribution of measured NEE (histogram with kernel density estimate), illustrating that most observations are concentrated around near-zero fluxes. The lower panel presents residuals (predicted − observed NEE) grouped into equal-width bins of measured NEE. Boxes represent the interquartile range (25th–75th percentiles) with the median indicated, while whiskers denote the 5th and 95th percentiles; the dashed horizontal line marks zero residual.

In the lower panel, boxes represent the interquartile range (25th–75th percentiles) of residuals within each measured-NEE bin, with the median indicated. Whiskers denote the 5th and 95th percentiles, thereby characterising the central 90 % of residuals and avoiding undue influence from isolated extreme values. The dashed horizontal line indicates zero residual.

Residuals are tightly distributed around zero for near-zero measured NEE, which corresponds to the dominant regime in the data. This indicates high predictive skill in the most frequently occurring conditions and explains the high overall Nash–Sutcliffe efficiency. With increasing absolute NEE values, both the median residual and the 5th–95th percentile range progressively deviate from zero, indicating a systematic damping of extreme flux magnitudes by the model. This behaviour is approximately monotonic across the flux range and reflects a regime-dependent bias rather than sporadic outliers.

The asymmetry and widening of the 5th–95th percentile range at large flux magnitudes demonstrate that model uncertainty increases primarily in rarely observed regimes. Consequently, the reduced regression slope observed in the joint distribution arises from conservative predictions at extreme uptake and release, rather than from poor overall model performance. This diagnostic highlights that global performance metrics are dominated by the dense near-zero flux regime, whereas residual structure at the extremes reveals limitations in representing large-magnitude fluxes.

Appendix C: Annual Budgets - Summary

https://doi.org/10.5194/egusphere-2026-3151
Preprint. Discussion started: 24 June 2026
© Author(s) 2026. CC BY 4.0 License.

Table C1. Annual CO_2 budgets. Carbon exports include harvested biomass and dissolved organic carbon losses expressed as CO_2 equivalents associated with water pumping, whereas imports represent manure applications. All fluxes are reported in t_{CO_2} (ha yr)$^{-1}$. Harvest exports for ASD_MP are reported as zero because no field harvest records were available for this site during the measurement period; this differs from chamber-based harvest estimates reported by Aben et al. (2024) for the same site, which reflect a different quantification methodology.

location	year	NEE_mean	Imports	Exports	NECB	NEE_std
ALB_MS	2022	6.42	2.03	10.70	15.10	8.71
ALB_MS	2023	1.90	3.93	18.30	16.27	8.47
ALB_RF	2022	2.57	2.03	9.92	10.46	9.53
ALB_RF	2023	-5.54	2.36	10.50	2.60	10.90
AMM	2022	23.79	6.51	16.50	33.78	15.20
AMM	2023	18.34	6.51	0.00	11.83	8.20
AMR	2022	15.23	6.51	16.50	25.22	9.21
AMR	2023	20.08	6.51	0.00	13.56	7.50
ANK_PT	2022	-9.63	0.00	6.50	-3.13	5.89
ASD_MP	2022	-1.05	0.00	0.00	-1.05	4.98
ASD_MP	2023	-2.16	0.00	0.00	-2.16	5.05
BUO	2022	-16.28	3.84	5.87	-14.25	7.57
BUO	2023	-17.71	3.84	0.00	-21.55	6.45
BUW	2022	-6.64	3.84	0.00	-10.47	9.01
BUW	2023	-10.97	3.84	0.00	-14.80	4.23
CAM	2021	-5.41	0.00	0.00	-5.41	5.70
CAM	2022	-13.64	0.00	0.00	-13.64	6.22
CAM	2023	-11.48	0.00	0.00	-11.48	6.93
DEM	2023	3.35	0.00	0.76	4.11	4.99
HOC	2022	-6.01	2.82	12.95	4.12	7.99
HOC	2023	-3.13	8.53	14.85	3.19	8.36
HOH	2022	-5.89	2.90	15.56	6.76	11.00
HOH	2023	-0.02	3.68	12.73	9.03	13.20
ILP_PT	2022	-9.08	0.00	0.00	-9.08	2.55
ILP_PT	2023	-6.34	0.00	0.00	-6.34	2.21
LAW_MS_ICOS	2022	1.36	6.98	11.35	5.72	4.24
LAW_MS_ICOS	2023	-0.96	6.73	9.93	2.25	5.14
LAW_MS_MOBmob_ec01	2022	-1.96	6.98	11.35	2.40	4.35
LDC	2022	17.79	2.03	10.72	26.48	10.40

continued on next page

https://doi.org/10.5194/egusphere-2026-3151
Preprint. Discussion started: 24 June 2026
© Author(s) 2026. CC BY 4.0 License.

Table C1 – continued from previous page

location	year	NEE_mean	Imports	Exports	NECB	NEE_std
LDC	2023	-1.27	2.03	10.72	7.42	8.49
LDH	2022	0.71	2.03	10.72	9.40	8.20
LDH	2023	-11.24	2.03	10.72	-2.55	7.87
ONL	2021	-6.27	0.00	0.00	-6.27	2.81
ONL	2022	-3.46	0.00	0.00	-3.46	3.13
ONL	2023	-2.96	0.00	0.00	-2.96	4.32
WRW_OW	2022	12.89	0.00	0.00	12.89	3.56
WRW_OW	2023	10.45	0.00	0.00	10.45	3.25
WRW_SR	2022	-7.29	0.00	0.00	-7.29	3.84
WRW_SR	2023	-12.10	0.00	0.00	-12.10	2.79
ZEG_PT	2021	-4.67	0.00	12.90	8.23	4.20
ZEG_PT	2022	-8.19	0.00	7.80	-0.39	4.68

https://doi.org/10.5194/egusphere-2026-3151
Preprint. Discussion started: 24 June 2026
© Author(s) 2026. CC BY 4.0 License.

Appendix D: Mobile Mast - Configuration

Fig. D1. Compact eddy covariance (EC) system installed in managed peat grassland. The setup includes a three-dimensional sonic anemometer and an enclosed infrared gas analyzer mounted on a stabilized mast, with data logging and power supply units.

The EC configuration shown here is designed for parcel-scale flux measurements in low-stature peatland vegetation. The relatively low measurement height enhances sensitivity to local surface conditions and management effects, while guy wires ensure mast stability under exposed field conditions. The system enables high-frequency measurements of wind components and greenhouse gas concentrations for estimating turbulent carbon and energy fluxes.

https://doi.org/10.5194/egusphere-2026-3151
Preprint. Discussion started: 24 June 2026
© Author(s) 2026. CC BY 4.0 License.

Appendix E: Standard Equipment

Table E1. Standard meteorological instrumentation set in NOBV. *sensor only used as backup in Fryslân network

Variables	Instrument make and type	Implementation
Temperature, RH, windspeed, wind direction, pressure	Gill maximet GMX500	2 m high top of mast
Incoming and reflected, shortwave and longwave radiation	Apogee SN-500 and Hukseflux SR05*	2 m height and 1.5 m away from mast
Incoming and reflected PAR and NIR	Skye SKR1840D/ND	2 m and 1.5 m away from mast
Soil heat flux	Hukseflux HFP01	2 x at 5 cm depth
Soil moisture and temperature	SENTEK Drill&Drop 120 cm	0-120 cm depth
Precipitation	ARG314	On ground
Groundwater table	Ellitrack-D	Several locations

Appendix F: CO_2 Import/export - Manure application and Harvest

The grazing influence is for now neglected in the data analysis process, our information about grazing period and the density of cattle in the studied pastures was judged too coarse. Grazing is assumed to have an approximately neutral effect on annual carbon balance at the parcel scale, since the carbon consumed by livestock is largely returned as excreta within the same footprint area. This is a simplification of reality — in practice, a fraction of consumed carbon leaves the parcel via animal products, respiration, and methane, and grazing events are incompletely captured by mobile EC setups — representing a known source of uncertainty in NECB estimates for grazed sites. However, we made an attempt to estimate the amount of CO_2 represented as an input via manure application and exports through harvest.

In each case the literature provides conversion coefficients to estimate the amount of carbon subtracted/added to the ecosystem, which can be easily converted to CO_2 amounts via Eq. F1.

$$k_i = \frac{44}{12} f_{\text{dry}-C} f_{\text{dry}} \tag{F1}$$

F_{manure} is computed from two variables, the liquid manure volume (v_{liq}) and the mass of solid manure applied (m_{sol}). $F_{harvest}$ is computed from v_{harv} the volume harvest. Simplified models are considered, either assuming that manure has a fixed total amount of Carbon and similar to (Kamilaris et al., 2020), either by considering that vegetation has a fixed dried mass and a fixed carbon ratio (0.45) for the estimated dry mass (Garnier and Vancaeyzeele, 1994).

https://doi.org/10.5194/egusphere-2026-3151
Preprint. Discussion started: 24 June 2026
© Author(s) 2026. CC BY 4.0 License.

$$\mathrm{F_{manure}} = \frac{1}{S_{pasture}} \left(k_{\mathrm{liq}} \sum_i v_{liq-i} + k_{sol} \sum_i m_{sol-i} \right) \tag{F2}$$

$$F_{\mathrm{harvest}} = \frac{1}{S_{pasture}} \, k_{\mathrm{harvest}} \, m_{\mathrm{harv,dry}} \tag{F3}$$

The conversion coefficients used in this report are summarised in Table F1.

Table F1. Conversion coefficient - Import/export

$k_{\mathrm{liq}}(\mathrm{kg_{CO_2}\ ha^{-1}\ m^{-3}})$	$k_{sol}(\mathrm{kg_{CO_2}\ ha^{-1}\ t^{-1}})$	$k_{\mathrm{harvest}}(\mathrm{kg_{CO_2}\ ha^{-1}\ kg_{dry}^{-1}})$
0.13	6.42×10^{-4}	1.57

Code and data availability. The annual CO_2 budget totals analysed in this study are reported in full in the appendix tables. The underlying eddy-covariance flux datasets are being prepared for open publication as part of a dedicated data paper (Zhao et al., in preparation); until that publication, data are available from the corresponding author upon reasonable request. Gap-filling using the Marginal Distribution Sampling method was performed with the REddyProc R package (Wutzler et al., 2018). The machine-learning processing pipeline is still under active development and will be made available upon request.

Author contributions. BK, RH, and LB guided the scientific process, which was carried out by LB. BK and LB conceived the study. LB developed the methodology, performed the formal analysis and gap-filling, produced the figures, and wrote the original draft. AB and QvG contributed to the methodology and developed the processing software, with WF, JB, and HB also contributing to software development and data curation; AB additionally curated the flux data and carried out validation. WJ, TH, RL, and MvdB were responsible for the eddy-covariance measurement sites and provided field resources, supported by RN, NB, and YvdV in field operations. HZ curated the flux datasets being prepared for open publication. NB, YvdV, and CF administered the project; BK, CF, and RH provided supervision; and RH acquired funding. BK, AB, GE, and RH contributed to manuscript revisions.

Competing interests. The contact author has declared that none of the authors has any competing interests.

Acknowledgements. This research was conducted within the framework of the Netherlands Research Programme on Greenhouse Gas Dynamics in Peatlands and Organic Soils (NOBV). We gratefully acknowledge the contributions of all consortium partners for their support, data provision, and scientific discussions, in particular the collaboration with regional water authorities, including Wetterskip Fryslân, and nature conservation organisations such as Natuurmonumenten. We also thank colleagues and collaborators for valuable feedback throughout the development of this work. Language editing and stylistic improvements were assisted using Grammarly, and OpenAI's ChatGPT was used

https://doi.org/10.5194/egusphere-2026-3151
Preprint. Discussion started: 24 June 2026
© Author(s) 2026. CC BY 4.0 License.

to support drafting and refinement of the manuscript text; all scientific content, analyses, and interpretations remain the sole responsibility of the authors.

We gratefully acknowledge Ignacio Kovacevic Andueza, Jeferson Zerrudo, Corine Van Huissteden, and Ruchita Ingle for their valuable contributions, discussions, and support throughout this work. We gratefully acknowledge Tan Lippman, Freek Engel, and Laura van der Poel for their thorough review of this manuscript and their valuable and constructive comments.

Financial support. This research has been supported by the Netherlands Research Programme on Greenhouse Gas Dynamics in Peatlands and Organic Soils (NOBV), funded by the Dutch Ministry of Agriculture, Fisheries, Food Security and Nature and directed by the Foundation for Applied Water Research (STOWA). Additional funds were received from Provincie Fryslân.

https://doi.org/10.5194/egusphere-2026-3151
Preprint. Discussion started: 24 June 2026
© Author(s) 2026. CC BY 4.0 License.

References

Aben, R. C. H., van de Craats, D., Boonman, J., Peeters, S. H., Vriend, B., Boonman, C. C. F., van der Velde, Y., Erkens, G., and van den Berg, M.: CO2 emissions of drained coastal peatlands in the Netherlands and potential emission reduction by water infiltration systems, Biogeosciences, 21, 4099–4118, https://doi.org/10.5194/bg-21-4099-2024, 2024.

Arets, E., van Baren, S., Hendriks, C., Kramer, H., Lesschen, J., and Schelhaas, M.: Greenhouse gas reporting of the LULUCF sector in the Netherlands: methodological background, update 2023, Tech. rep., Wettelijke Onderzoekstaken Natuur & Milieu, https://doi.org/10.18174/588942, 2023.

Aubinet, M., Vesala, T., and Papale, D., eds.: Eddy Covariance: A Practical Guide to Measurement and Data Analysis, Springer Netherlands, https://doi.org/10.1007/978-94-007-2351-1, 2012.

Bechtold, M., Tiemeyer, B., Laggner, A., Leppelt, T., Frahm, E., and Belting, S.: Large-scale regionalization of water table depth in peatlands optimized for greenhouse gas emission upscaling, Hydrology and Earth System Sciences, 18, 3319–3339, https://doi.org/10.5194/hess-18-3319-2014, 2014.

Buzacott, A. J. V., Kruijt, B., Bataille, L., van Giersbergen, Q., Heuts, T. S., Fritz, C., Nouta, R., Erkens, G., Boonman, J., van den Berg, M., van Huissteden, J., and van der Velde, Y.: Drivers and Annual Totals of Methane Emissions From Dutch Peatlands, Global Change Biology, 30, https://doi.org/10.1111/gcb.17590, 2024.

Chan, P. and van den Akker, J.: Bodemdaling door veenoxidatie : Broeikasgasemissies in veenweidegebied, waar hebben we het over?, Bodem, 32, 6–8, https://edepot.wur.nl/651766, accessed via Wageningen University & Research eDepot, 2022.

Chen, T. and Guestrin, C.: XGBoost: A Scalable Tree Boosting System, in: Proceedings of the 22nd ACM SIGKDD International Conference on Knowledge Discovery and Data Mining, pp. 785–794, https://doi.org/10.1145/2939672.2939785, 2016.

Couwenberg, J.: Some facts on submerged drains in Dutch peat pastures, Tech. rep., 2018.

Dumortier, P., Motte, L. G. d. l., Andriamandroso, A., Aubinet, M., Beckers, Y., Bindelle, J., Cock, N. D., Lebeau, F., and Heinesch, B.: Beef cattle methane emission estimation using the eddy covariance technique in combination with geolocation, Agricultural and Forest Meteorology, 297, 108 249, https://doi.org/10.1016/j.agrformet.2020.108249, 2021.

Erkens, G., van der Meulen, M. J., and Middelkoop, H.: Double trouble: subsidence and CO2 respiration due to 1, 000 years of Dutch coastal peatlands cultivation, Hydrogeology Journal, 24, 551–568, https://doi.org/10.1007/s10040-016-1380-4, 2016.

Erkens, G., Melman, R., Jansen, S., Boonman, J., Hefting, M., Keuskamp, J., Bootsma, H., Nougues, L., Van Den Berg, M., Van Der Velde, Y., Van Den Akker, J., Hessel, R., Fritz, C., Aben, R., Kruijt, B., Hutjes, R., Faye Harpenslager, S., Van Asselen, S., Hommes, S., and Kooi, H.: Subsurface Organic Matter Emission Registration System (SOMERS) SOMERS: Subsurface Organic Matter Emission Registration System Beschrijving SOMERS 1.0, onderliggende modellen en veenweidenrekenregels, Tech. rep., 2022.

Evans, C. D., Peacock, M., Baird, A. J., Artz, R. R. E., Burden, A., Callaghan, N., Chapman, P. J., Cooper, H. M., Coyle, M., Craig, E., Cumming, A., Dixon, S., Gauci, V., Grayson, R. P., Helfter, C., Heppell, C. M., Holden, J., Jones, D. L., Kaduk, J., Levy, P., Matthews, R., McNamara, N. P., Misselbrook, T., Oakley, S., Page, S. E., Rayment, M., Ridley, L. M., Stanley, K. M., Williamson, J. L., Worrall, F., and Morrison, R.: Overriding water table control on managed peatland greenhouse gas emissions, Nature, 593, 548–552, https://doi.org/10.1038/s41586-021-03523-1, 2021.

Falge, E., Baldocchi, D., Tenhunen, J., Aubinet, M., Bakwin, P., Berbigier, P., Bernhofer, C., Burba, G., Clement, R., Davis, K. J., Elbers, J. A., Goldstein, A. H., Grelle, A., Granier, A., Guðmundsson, J., Hollinger, D., Kowalski, A. S., Katul, G., Law, B. E., Malhi, Y., Meyers, T., Monson, R. K., Munger, J., Oechel, W., U, K. T. P., Pilegaard, K., Üllar Rannik, Rebmann, C., Suyker, A., Valentini, R., Wilson, K.,

https://doi.org/10.5194/egusphere-2026-3151
Preprint. Discussion started: 24 June 2026
© Author(s) 2026. CC BY 4.0 License.

and Wofsy, S.: Seasonality of ecosystem respiration and gross primary production as derived from FLUXNET measurements, Agricultural and Forest Meteorology, 113, 53–74, https://doi.org/10.1016/s0168-1923(02)00102-8, 2002.

Foken, T., Göockede, M., Mauder, M., Mahrt, L., Amiro, B., and Munger, W.: Post-Field Data Quality Control, in: Handbook of Micrometeorology, pp. 181–208, Kluwer Academic Publishers, https://doi.org/10.1007/1-4020-2265-4_9, 2004.

Garnier, E. and Vancaeyzeele, S.: Carbon and nitrogen content of congeneric annual and perennial grass species: relationships with growth, Plant, Cell & Environment, 17, 399–407, https://doi.org/https://doi.org/10.1111/j.1365-3040.1994.tb00308.x, 1994.

Gebhardt, S., Fleige, H., and Horn, R.: Shrinkage processes of a drained riparian peatland with subsidence morphology, Journal of Soils and Sediments, 10, 484–493, https://doi.org/10.1007/s11368-009-0130-9, 2009.

Haentjens, N.: pylr2: Linear Regression Type II Models, https://doi.org/10.5281/zenodo.XXXXXXX, python package, MIT License, 2018.

Hoover, D. L. and Rogers, B. M.: Not all droughts are created equal: the impacts of interannual drought pattern and magnitude on grassland carbon cycling, Global Change Biology, 22, 1809–1820, https://doi.org/10.1111/gcb.13161, 2016.

Jacobs, C. M. J., Jacobs, A. F. G., Bosveld, F. C., Hendriks, D. M. D., Hensen, A., Kroon, P. S., Moors, E. J., Nol, L., Schrier-Uijl, A., and Veenendaal, E. M.: Variability of annual CO2 exchange from Dutch grasslands, Biogeosciences, 4, 803–816, https://doi.org/10.5194/bg-4-803-2007, 2007.

Joosten, E. W. W. C. S. H., ed.: Schweizerbart Science Publishers, Stuttgart, Germany, http://www.schweizerbart.de//publications/detail/isbn/9783510652839/Wichtmann_Schroder_Joosten_Paludicu, 2016.

Jurasinski, G., Günther, A., Huth, V., Couwenberg, J., and Glatzel, S.: chap. Greenhouse gas emissions, in: Joosten (2016), http://www.schweizerbart.de//publications/detail/isbn/9783510652839/Wichtmann_Schroder_Joosten_Paludicu, 2016.

Kamilaris, A., Mesa, I. F., Savé, R., Herralde, F. D., and Prenafeta-Boldú, F. X.: Can Animal Manure Be Used to Increase Soil Organic Carbon Stocks in the Mediterranean as a Mitigation Climate Change Strategy?, in: Progress in IS, pp. 227–241, Springer International Publishing, https://doi.org/10.1007/978-3-030-61969-5_16, 2020.

Kechavarzi, C., Dawson, Q., Bartlett, M. S., and Leeds-Harrison, P.: The role of soil moisture, temperature and nutrient amendment on co2 efflux from agricultural peat soil microcosms, Geoderma, 154, 203–210, https://doi.org/10.1016/j.geoderma.2009.02.018, 2010.

Kljun, N., Calanca, P., Rotach, M. W., and Schmid, H. P.: A simple two-dimensional parameterisation for Flux Footprint Prediction (FFP), Geoscientific Model Development, 8, 3695–3713, https://doi.org/10.5194/gmd-8-3695-2015, 2015.

Koch, J., Elsgaard, L., Greve, M. H., Gyldenkærne, S., Hermansen, C., Levin, G., Wu, S., and Stisen, S.: Water-table-driven greenhouse gas emission estimates guide peatland restoration at national scale, Biogeosciences, 20, 2387–2403, https://doi.org/10.5194/bg-20-2387-2023, 2023.

Kwon, M. J., Ballantyne, A., Ciais, P., Qiu, C., Salmon, E., Raoult, N., Guenet, B., Göckede, M., Euskirchen, E. S., Nykänen, H., Schuur, E. A. G., Turetsky, M. R., Dieleman, C. M., Kane, E. S., and Zona, D.: Lowering water table reduces carbon sink strength and carbon stocks in northern peatlands, Global Change Biology, 28, 6752–6770, https://doi.org/https://doi.org/10.1111/gcb.16394, 2022.

McDermitt, D., Burba, G., Xu, L., Anderson, T., Komissarov, A., Riensche, B., Schedlbauer, J., Starr, G., Zona, D., Oechel, W., Oberbauer, S., and Hastings, S.: A new low-power, open-path instrument for measuring methane flux by eddy covariance, Applied Physics B, 102, 391–405, https://doi.org/10.1007/s00340-010-4307-0, 2010.

Ministerie van Economische Zaken en Klimaat: Klimaatakkoord, Government report, 2019.

Moffat, A. M., Papale, D., Reichstein, M., Hollinger, D. Y., Richardson, A. D., Barr, A. G., Beckstein, C., Braswell, B. H., Churkina, G., Desai, A. R., Falge, E., Gove, J. H., Heimann, M., Hui, D., Jarvis, A. J., Kattge, J., Noormets, A., and Stauch, V. J.: Comprehen-

https://doi.org/10.5194/egusphere-2026-3151
Preprint. Discussion started: 24 June 2026
© Author(s) 2026. CC BY 4.0 License.

sive comparison of gap-filling techniques for eddy covariance net carbon fluxes, Agricultural and Forest Meteorology, 147, 209–232, https://doi.org/10.1016/j.agrformet.2007.08.011, 2007.

Moncrieff, J., Massheder, J., de Bruin, H., Elbers, J., Friborg, T., Heusinkveld, B., Kabat, P., Scott, S., Soegaard, H., and Verhoef, A.: A system to measure surface fluxes of momentum, sensible heat, water vapour and carbon dioxide, Journal of Hydrology, 188-189, 589–611, https://doi.org/10.1016/s0022-1694(96)03194-0, 1997.

Moncrieff, J., Clement, R., Finnigan, J., and Meyers, T.: Averaging, Detrending, and Filtering of Eddy Covariance Time Series, pp. 7–31, Springer Netherlands, Dordrecht, https://doi.org/10.1007/1-4020-2265-4_2, 2004.

Nijman, T. P., van Giersbergen, Q., Heuts, T. S., Nouta, R., Boonman, C. C., Velthuis, M., Kruijt, B., Aben, R. C., and Fritz, C.: Drainage effects on carbon budgets of degraded peatlands in the north of the Netherlands, Science of The Total Environment, 935, 172 882, https://doi.org/10.1016/j.scitotenv.2024.172882, 2024.

Papale, D., Reichstein, M., Aubinet, M., Canfora, E., Bernhofer, C., Kutsch, W., Longdoz, B., Rambal, S., Valentini, R., Vesala, T., and Yakir, D.: Towards a standardized processing of Net Ecosystem Exchange measured with eddy covariance technique: algorithms and uncertainty estimation, Biogeosciences, 3, 571–583, https://doi.org/10.5194/bg-3-571-2006, 2006.

Pijlman, J., Roelen, S., and Eekeren, N. V.: Klimaatmaatregelen in het veenweidegebied in relatie tot biodiversiteit, bodem-en waterkwaliteit Een inventarisatie van effecten, Tech. rep., www.louisbolk.nl/publicaties, 2020.

Preston, M. D., Smemo, K. A., McLaughlin, J. W., and Basiliko, N.: Peatland microbial communities and decomposition processes in the james bay lowlands, canada, Frontiers in Microbiology, 3, https://doi.org/10.3389/fmicb.2012.00070, 2012.

Reichstein, M., Falge, E., Baldocchi, D., Papale, D., Aubinet, M., Berbigier, P., Bernhofer, C., Buchmann, N., Gilmanov, T., Granier, A., Grunwald, T., Havrankova, K., Ilvesniemi, H., Janous, D., Knohl, A., Laurila, T., Lohila, A., Loustau, D., Matteucci, G., Meyers, T., Miglietta, F., Ourcival, J.-M., Pumpanen, J., Rambal, S., Rotenberg, E., Sanz, M., Tenhunen, J., Seufert, G., Vaccari, F., Vesala, T., Yakir, D., and Valentini, R.: On the separation of net ecosystem exchange into assimilation and ecosystem respiration: review and improved algorithm, Global Change Biology, 11, 1424–1439, https://doi.org/10.1111/j.1365-2486.2005.001002.x, 2005.

Schrier-Uijl, A. P., Kroon, P. S., Hensen, A., Leffelaar, P. A., Berendse, F., and Veenendaal, E. M.: Comparison of chamber and eddy covariance-based CO2 and CH4 emission estimates in a heterogeneous grass ecosystem on peat, Agricultural and Forest Meteorology, 150, 825–831, https://doi.org/10.1016/j.agrformet.2009.11.007, 2010.

Schrier-Uijl, A. P., Kroon, P. S., Hendriks, D. M. D., Hensen, A., Van Huissteden, J., Berendse, F., and Veenendaal, E. M.: Agricultural peatlands: towards a greenhouse gas sink – a synthesis of a Dutch landscape study, Biogeosciences, 11, 4559–4576, https://doi.org/10.5194/bg-11-4559-2014, 2014.

Sen, S., Verhoeven, D., and Weikard, H.-P.: Sinking Land: Optimal Control of Subsidence, SSRN Electronic Journal, https://doi.org/10.2139/ssrn.4608805, 2023.

Shao, J., Zhou, X., Luo, Y., Li, B., Aurela, M., Billesbach, D., Blanken, P. D., Bracho, R., Chen, J., Fischer, M., Fu, Y., and Gu, L.: Biotic and climatic controls on interannual variability in carbon fluxes across terrestrial ecosystems, Agricultural and Forest Meteorology, 205, 11–22, https://doi.org/10.1016/j.agrformet.2015.02.007, 2015.

Song, Y., Song, C., Hou, A., Sun, L., Wang, X., Ma, X., Jiang, L., Liu, C., and Gao, J.: Temperature, soil moisture, and microbial controls on co2 and ch4 emissions from a permafrost peatland, Environmental Progress & Sustainable Energy, 40, https://doi.org/10.1002/ep.13693, 2021.

Tiemeyer, B., Borraz, E. A., Augustin, J., Bechtold, M., Beetz, S., Beyer, C., Drösler, M., Ebli, M., Eickenscheidt, T., Fiedler, S., Förster, C., Freibauer, A., Giebels, M., Glatzel, S., Heinichen, J., Hoffmann, M., Höper, H., Jurasinski, G., Leiber-Sauheitl, K., Peichl-Brak, M.,

https://doi.org/10.5194/egusphere-2026-3151
Preprint. Discussion started: 24 June 2026
© Author(s) 2026. CC BY 4.0 License.

Roßkopf, N., Sommer, M., and Zeitz, J.: High emissions of greenhouse gases from grasslands on peat and other organic soils, Global Change Biology, 22, 4134–4149, https://doi.org/10.1111/gcb.13303, 2016.

Tiemeyer, B., Freibauer, A., Borraz, E. A., Augustin, J., Bechtold, M., Beetz, S., Beyer, C., Ebli, M., Eickenscheidt, T., Fiedler, S., Förster, C., Gensior, A., Giebels, M., Glatzel, S., Heinichen, J., Hoffmann, M., Höper, H., Jurasinski, G., Laggner, A., Leiber-Sauheitl, K., Peichl-Brak, M., and Drösler, M.: A new methodology for organic soils in national greenhouse gas inventories: Data synthesis, derivation and application, Ecological Indicators, 109, 105 838, https://doi.org/10.1016/j.ecolind.2019.105838, 2020.

Tolunay, D., Kowalchuk, G. A., Erkens, G., and Hefting, M. M.: Aerobic and Anaerobic Decomposition Rates in Drained Peatlands: Impact of Botanical Composition, Science of The Total Environment, 930, 172 639, https://doi.org/10.1016/j.scitotenv.2024.172639, 2024.

van Agtmaal, M., Keuskamp, J., and Hefting, M.: Peat enrichment with clay minerals to reduce CO2 emissions: a proof of principle study, https://doi.org/10.5194/egusphere-egu25-19848, 2025.

van den Akker, J., Kuikman, P. J., de Vries, F. P., Hoving, I., Pleijter, M., Hendriks, R. F. A., Wolleswinkel, R. J., Simões, R., and Kwakernaak, C.: Emission of CO2 from agricultural peat soils in the Netherlands and ways to limit this emission, 2010.

van den Akker, J., Querner, E., Jansen, P., and Kwakernaak, C.: Analysing water level strategies to reduce soil subsidence in Dutch peat meadows, Journal of Hydrology, 446-447, 59–69, https://doi.org/10.1016/j.jhydrol.2012.04.029, 2012.

van der Poel, L. M., Bataille, L. V., Kruijt, B., Franssen, W., Jans, W., Biermann, J., Rietman, A., Buzacott, A. J. V., van der Velde, Y., Boelens, R., and Hutjes, R. W. A.: Groundwater-CO2 Emissions Relationship in Dutch Peatlands Derived by Machine Learning Using Airborne and Ground-Based Eddy Covariance Data, https://doi.org/10.5194/egusphere-2025-431, 2025.

Veenendaal, E. M., Kolle, O., Leffelaar, P. A., Schrier-Uijl, A. P., Van Huissteden, J., Van Walsem, J., Möller, F., and Berendse, F.: CO_2 exchange and carbon balance in two grassland sites on eutrophic drained peat soils, Biogeosciences, 4, 1027–1040, https://doi.org/10.5194/bg-4-1027-2007, 2007.

Vekuri, H., Tuovinen, J.-P., Kulmala, L., Aurela, M., Thum, T., Liski, J., and Lohila, A.: Improved uncertainty estimates for eddy covariance-based carbon dioxide balances using deep ensembles for gap-filling, Agricultural and Forest Meteorology, 371, 110 558, https://doi.org/10.1016/j.agrformet.2025.110558, 2025.

Vickers, D. and Mahrt, L.: Quality Control and Flux Sampling Problems for Tower and Aircraft Data, Journal of Atmospheric and Oceanic Technology, 14, 512–526, https://doi.org/10.1175/1520-0426(1997)014<0512:qcafsp>2.0.co;2, 1997.

Vos, P. L., Vos, P., Meulen, M. J. v. d., Weerts, H., Weerts, H., and Bazelmans: Atlas of the Holocene Netherlands, https://doi.org/10.5117/9789463724432, 2020.

Webb, E. K., Pearman, G. I., and Leuning, R.: Correction of flux measurements for density effects due to heat and water vapour transfer, Quarterly Journal of the Royal Meteorological Society, 106, 85–100, https://doi.org/10.1002/qj.49710644707, 1980.

Weideveld, S. T. J., Liu, W., Berg, M. V. D., Lamers, L. P. M., and Fritz, C.: Conventional subsoil irrigation techniques do not lower carbon emissions from drained peat meadows, Biogeosciences, 18, 3881–3902, https://doi.org/10.5194/bg-18-3881-2021, 2021.

Wils, T. H., van den Akker, J. J., Korff, M., Bakema, G., Hegger, D. L., Hessel, R., van den Ende, M. A., van Gils, M. M., and Verstand, D.: Measures to reduce land subsidence and greenhouse gas emissions in peatlands: A Dutch case study, Land Use Policy, 152, https://doi.org/10.1016/j.landusepol.2025.107500, 2025.

Woestenburg, M. and Kwakernaak, C.: Waarheen met het veen. Kennis voor keuzes in het westelijke veenweidegebied, Tech. rep., Wageningen: Landwerk., 2009.

https://doi.org/10.5194/egusphere-2026-3151
Preprint. Discussion started: 24 June 2026
© Author(s) 2026. CC BY 4.0 License.

Wutzler, T., Lucas-Moffat, A., Migliavacca, M., Knauer, J., Sickel, K., Šigut, L., Menzer, O., and Reichstein, M.: Basic and extensible post-processing of eddy covariance flux data with REddyProc, Biogeosciences, 15, 5015–5030, https://doi.org/10.5194/bg-15-5015-2018, 2018.

Zingstra, H. and Vertegaal, P.: Natural Climate Buffers: Promising Examples of Nature Based Solutions, Nature-Based Solutions ieri, oggi e domani, p. 27, 2021.